Flow Time in Collaborative Assembly Systems: Performance Evaluation, System Properties, and Case Study

Authors

September 3, 2020

Abstract

In this paper, an analytical method is introduced to evaluate the flow time of assembly systems with collaborative robots. In such a system, an operator and a collaborative robot can independently carry out preparation tasks first, then they work jointly to finish the assembly operations. To study the productivity performance of these systems, a stochastic process model is developed, where the joint work is modeled as an assembly merge process, and the task times of all operation processes are described by phase-type distributions. Closed-form solutions of system performance, such as flow time expectation and variability, as well as service rate, are derived analytically. The system properties of monotonicity, work allocation, and bottleneck identification are investigated. In addition, a case study is introduced to evaluate the performance of a front panel assembly process in automotive manufacturing.

Keywords: Assembly system, collaborative robots, flow time, service rate, phase-type distribution.

1 Introduction

Manufacturing industry is now facing tremendous challenges. In order to continuously improve productivity, quality, sustainability, and customer satisfaction throughout the product life cycle, both industrial automation to maintain high efficiency and repeatability, and operation flexibility to deal with customization and variability are of critical importance, and should be balanced to ensure competitiveness. In responding to such challenges, in recent years, there has been an increasing trend to use collaborative robots in assembly systems. The collaborative robot market share has been growing significantly. It is projected that the global market will grow from USD 981 million in 2020 to USD 7,972 billion by 2026 (Collaborative Robots Market Research Report (2020)). Thus, collaborative assembly systems are gradually becoming an important element of smart manufacturing and factory automation, particularly beneficial to small- and medium-sized manufacturing enterprises (Marvel (2014)).

In a collaborative assembly system, the human operators and the robots share the same workspace and collaborate safely on a variety of tasks, such as pick-and-place, assembly, screwing, material handling, and inspection. Such robots are often referred to as collaborative robots or cobots. To address the collaborative assembly systems with cobots, many surveys and numerous studies on human robot collaborations have been conducted to discuss the issues and challenges, such as the concept, foundational framework, and various uses of cobots (Chandrasekaran and Conrad (2015); Djuric *et al.* (2016)), the safety, interfaces, and applications in industrial settings (Lasota *et al.* (2017); Villani *et al.* (2018)), the enabling technologies for collaborations (Bauer *et al.* (2008); Bolmsjo *et al.* (2012)), and cobot programming (El Zaatari *et al.* (2019)).

From an assembly system perspective, production planning and scheduling are of significant importance. Thus, traditional research problems, such as line balancing (Mura and Dini (2019); Weckenborg *et al.* (2020), sequencing and task assignment (Maganha *et al.* (2019); Tsarouchi *et al.* (2017); Faccio *et al.* (2019)), have attracted many research attentions under the collaborative robots environment. Many cobot scheduling studies consider makespan as an important measurement, and develop optimization models by considering cost, safety, strain index, logistic constraints and product characteristics, etc., to minimize makespans (e.g., Chen *et al.* (2013); Zanchettin *et al.* (2015); Pearce *et al.* (2018); Faccio *et al.* (2020); Mokhtarzadeh *et al.* (2020)). However, most of the works on collaborative robot systems focus on design and programming of

cobots, or task allocation between robots and human operators, using detailed kinematics and aggregated task time, or assuming sequential process of tasks.

In spite of the available studies, modeling and analysis of collaborative assembly systems are still in an infant phase. Less research has been paid to evaluate the productivity or time performance of the cobot systems with both independent and collaborative features. Consider the following collaborative assembly scenario: The operators and the cobots first carry out preparation tasks independently, and then work jointly to finish the assembly process, as shown in Figure 1. Such systems can be widely observed in automotive, appliance, battery, and equipment manufacturing systems.

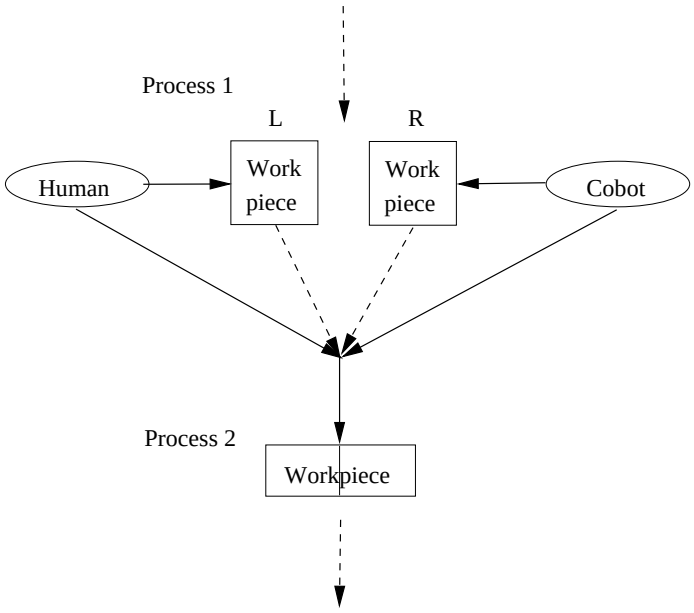

Figure 1: A collaborative scenario in an assembly system

To study such a collaborative assembly system, the activities and the associated task times should be modeled and analyzed explicitly. Particularly, as the productivity performance, such as flow time or throughput, is critical for manufacturing operations to maintain competitiveness, developing an analytical model to study the system flow time is necessary and important.

Although there exist numerous studies of time performance in queueing networks addressing split and merge structures, most of them tackles production merge, where parts from different routes go through the merging node sequentially (see, for instance, Altoik and Perros (1986); Tsimashenka and Knottenbelt (2011); Fiorini and Lipsky (2015)). Similar issues exist in stochastic PERT networks as well (e.g., Shih (2005)). However, in a collaborative assembly system (Figure 1), the merge process is an assembly merge, where parts from different routes are assembled or integrated into one single part). Modeling and analysis of assembly merge are much more complicated. Even though extensive research in manufacturing systems has been developed during the last three decades (see, for instance, monographs by Viswanadham and Narahari (1992); Buzacott and Shanthikumar (1993); Papadopoulos *et al.* (2014); Gershwin (1994); Li and Meerkov (2009), and reviews by Dallery and Gershwin (1992); Papadopoulos and Heavey (1996); Li *et al.* (2009); Papadopoulos *et al.* (2019)), most of the studies on assembly systems only address the mean time performance, and typically under Bernoulli or exponential assumption of processing times (see representative papers by Gershwin (1991); Chiang *et al.* (2000a,b); Li and Meerkov (2001); Helber and Justic (2004); Li (2005); Matta *et al.* (2005); Zhao and Li (2014); Jia *et al.* (2015); Ju *et al.* (2016)). As manual operations and robot downtimes in collaborative assembly systems can introduce significant variability in task times, the flow time in each process will vary with non-Markovian behavior and affect the assembly process and system performance in a nonlinear manner. Thus, not only the mean performance, but also the variability and complete distribution of flow time are important to ensure the desired productivity. Therefore, analytical models to accommodate more detailed activities, general distributions and higher order variability measures

are needed.

This paper is intended to contribute to this end by introducing a stochastic process model to analyze the flow time performance of such collaborative assembly systems. By assuming phase-type distribution of task processing time, a complete distribution of the process flow time is derived, and system properties, such as monotonicity, work allocation, and bottlenecks, are investigated. The goal of this study is not to focus on the cognitive or collaborative part of cobots (which is represented through processing times), but on the resulting flow time of the whole system. In addition, a case study at an automotive panel assembly process is introduced to illustrate the applicability of the study.

The rest of the paper is organized as follows: Section 2 introduces the model assumptions and formulates the problem. In Section 3, analytical methods with exponential and phase-type distribution task times are presented to evaluate system performance. The system properties are investigated in Section 4. A case study is described in Section 5. Finally, Section 6 summarizes the work. All proofs are provided in the Appendices.

2 System Description

Consider the collaborative assembly system with a human operator and a cobot illustrated in Figure 1. Such a system can be characterized by two independent preparation processes by the operator and cobot in parallel, respectively, and a joint process after assembly merge, as shown in Figure 2.

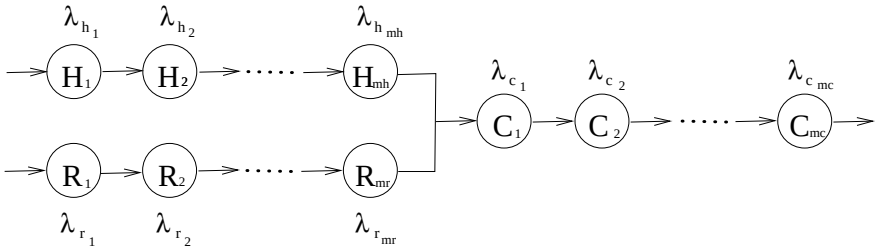

Figure 2: A collaborative assembly system

The following assumptions define the assembly system under study.

(i) The collaborative assembly system includes one cobot and one human operator.

(ii) The operator and cobot first work independently to carry out the preparation tasks. Afterwards, they work jointly to finish the assembly task. The joint process is an assembly merge process that can only start after both individual preparatory processes are finished.

(iii) The processes of individual preparation work of the cobot and the operator are described by random processes R and H, respectively, while the joint work process is characterized by a random process C.

(iv) Each random process, R, H, or C, is assumed to follow a phase-type distribution $f_i(t)$, $i = h, r, c$, which can represent the multiple consecutive steps in a process. In other words, there exist m_i phases, $i = h, r, c$, in process i, and each phase follows an exponential distribution with parameter $\lambda_{i,j}$, $j = 1, \ldots, m_i$, corresponding the multiple steps to finish the process task.

(v) The initial probability of each step in processes R, H, or C, is defined by $\alpha_{i,j}$, $i = h, r, c$, $j = 1, \ldots, m_i$, which can make the model applicable for general cases. Typically $\alpha_{i,1} = 1$ and all $\alpha_{i,j} = 0$, $j = 2, \ldots, m_i$, $i = h, r, c$.

Remark 1 As shown in Li and Meerkov (2005), the process time in most manufacturing environment has coefficient of variation (CV) smaller than 1. In addition, a process can always be decomposed into a series of steps, which corresponds to multiple phases in a phase-type distribution. Thus, assumption (iv) introduces phase-type distributions to characterize processes R, H and C, which can describe the non-Markovian feature and have $CV < 1$. To fit or approximate such processes, the parameters of the phase-type distribution can be obtained by using the empirical data (see Lang and Arthur (1996) for details). □

Remark 2 Although robot operation itself typically has few variability in processing time, the overall processing time may still be random due to unscheduled downtimes. Thus, for robot preparation process, a phase-type distribution is still assumed. Of course, by letting $\alpha_{r,j} = 0$, deterministic processing time can be obtained. □

Under assumptions (i)-(v), define the flow time to finish each process as t_k, $k = h, c, r$. Then the overall system flow time to finish the whole processes (i.e., the system flow time) can be defined as

$$t = \max(t_h, t_r) + t_c. \tag{1}$$

Then the expectation of flow time, T, needs to be evaluated. In addition to the average flow time, the variability, i.e., the coefficient of variation (CV), and whether the assembly system can finish the work on time are important performance measures as well, where the last one is usually referred to as flow time performance (FTP) or service rate, denoted as S. In this study, we define S as the probability to finish the whole process within a given time interval T_d. Therefore, we have

$$\begin{aligned} T &= E(t) \\ CV &= \frac{\sqrt{E[(t-T)^2]}}{T}, \\ S(T_d) &= P(t \le T_d). \end{aligned} \tag{2}$$

These measures are functions of all system parameters, m_i, λ_{ij}, $\alpha_{i,j}$, $i = h, r, c$, $j = 1, \ldots, m_i$. Then the problem to be studied in this paper can be formulated as: *Under assumptions (i)-(v), develop a method to evaluate the performance of the collaborative assembly system, i.e., calculate T, CV, and $S(T_d)$ as functions of system parameters, and investigate system properties.*

Solutions to the problem are introduced in Sections 3 and 4 below. In both sections, first, a special case of phase-type distribution, exponential distribution (i.e., 1 phase) models are studied, then we extend to more general phase-type distribution models.

3 Performance Evaluation

3.1 Analysis with Exponential Distribution Models

The exponential distribution only has 1 phase in a phase-type distribution, i.e., $m_i = 1$, $i = h, r, c$. The task time t_i, $i = h, r, c$, follows an exponential distribution with parameter λ_i. To completely describe the behavior of system flow time and meet the customer demands, it is necessary to know whether all the operations can be finished within a given time interval or not. Such a performance, referred to as service rate, is defined by the complete distribution of flow time. Thus, under the exponential distribution assumption, we first evaluate the service rate, i.e., the cumulative distribution function (CDF) of flow time.

Theorem 1 *Under assumptions (i)-(v) with 1 phase, i.e., $m_r = m_h = m_c = 1$, the system service rate for a given time period T_d, i.e., the CDF of flow time, can be calculated as*

$$S(T_d) = 1 - e^{-\lambda_c T_d} + \lambda_c(\gamma_{rh} - \gamma_r - \gamma_h), \tag{3}$$

where

$$\gamma_r = \begin{cases} \frac{e^{-\lambda_r T_d} - e^{-\lambda_c T_d}}{\lambda_c - \lambda_r}, & \text{if } \lambda_c \neq \lambda_r, \\ T_d e^{-\lambda_r T_d}, & o/w, \end{cases} \tag{4}$$

$$\gamma_h = \begin{cases} \frac{e^{-\lambda_h T_d} - e^{-\lambda_c T_d}}{\lambda_c - \lambda_h}, & \text{if } \lambda_c \neq \lambda_h, \\ T_d e^{-\lambda_h T_d}, & o/w, \end{cases} \tag{5}$$

$$\gamma_{rh} = \begin{cases} \frac{e^{-(\lambda_r+\lambda_h) T_d} - e^{-\lambda_c T_d}}{\lambda_c - \lambda_r - \lambda_h}, & \text{if } \lambda_c \neq \lambda_r + \lambda_h, \\ T_d e^{-(\lambda_r+\lambda_h) T_d}, & o/w. \end{cases} \tag{6}$$

Proof: See Appendix A. ∎

Using this result, the expected flow time can be evaluated.

Corollary 1 *Under assumptions (i)-(v) with 1 phase, i.e., $m_r = m_h = m_c = 1$, the expected flow time of the system can be calculated as*

$$T = \frac{1}{\lambda_c} + \frac{1}{\lambda_r} + \frac{1}{\lambda_h} - \frac{1}{\lambda_r + \lambda_h}. \tag{7}$$

Proof: See Appendix A. ∎

The first term in equation (7) represents the average task time of the joint process, while the last three terms characterize the maximum of task time of each preparation process, which can be understood as the preparation flow time needs to cover both individual processes and exclude the "overlapped part" (i.e., the term of $\lambda_r + \lambda_h$, which can be viewed as a combined rate).

Although the mean value is important, variability also impacts system performance significantly, particularly in a multi-process system, where one process's variation can cause the whole system unbalanced. However, variance itself cannot directly measure the impact of variability since it depends on the mean. Therefore, we calculate the ratio of standard deviation and the mean, i.e., the CV, of system flow time under exponential distribution assumption.

Corollary 2 *Under assumptions (i)-(v) with 1 phase, i.e., $m_r = m_h = m_c = 1$, the coefficient of variation of system flow time can be calculated as*

$$CV = \frac{\sqrt{\frac{1}{\lambda_h^2} + \frac{1}{\lambda_r^2} + \frac{1}{\lambda_c^2} - \frac{3}{(\lambda_r+\lambda_h)^2}}}{\frac{1}{\lambda_c} + \frac{1}{\lambda_r} + \frac{1}{\lambda_h} - \frac{1}{\lambda_r+\lambda_h}}. \tag{8}$$

Proof: See Appendix A. ∎

With these performance measures, the productivity of the collaborative assembly system can be quantified. Particularly, using these measurements, we can analyze the performance of each process explicitly, derive system properties, and use them to improve and optimize system performance.

3.2 Analysis with Phase-type Distribution Models

In practice, the work times may not follow exponential distributions, and many processes need to be finished in multiple steps. Thus, a more general case, the phase-type distribution model, is studied to represent the variability of the process and serial nature of multiple steps. Specifically, consider a random process, R, H, or C, with m_i, $i = h, r, c$, steps following exponential distributions. Then each process can be described by a continuous time Markov chain with $m_i + 1$ states, where the first m_i states are transient, and the last one is an absorbing state. To characterize such a process, a generator matrix $\boldsymbol{Q}_i$, $i = h, r, c$, can be defined as

$$\boldsymbol{Q}_i = \begin{bmatrix} \boldsymbol{B}_i & \boldsymbol{b}_i \\ \boldsymbol{0} & 0 \end{bmatrix}, \tag{9}$$

where matrix $\boldsymbol{B}_i$ and vector $\boldsymbol{b}_i$ are defined as

$$\boldsymbol{B}_i = \begin{bmatrix} -\lambda_{i,1} & \lambda_{i,1} & 0 & \cdots & 0 \\ 0 & -\lambda_{i,2} & \lambda_{i,2} & \ddots & 0 \\ 0 & \ddots & \ddots & \ddots & \vdots \\ 0 & \ddots & \ddots & -\lambda_{i,m_{i-1}} & \lambda_{i,m_{i-1}} \\ 0 & \ddots & \ddots & \ddots & -\lambda_{i,m_i} \end{bmatrix}, \tag{10}$$

$$\boldsymbol{b}_i = -\boldsymbol{B}_i \boldsymbol{1} = \begin{bmatrix} 0 \\ \vdots \\ \lambda_{i,m_i} \end{bmatrix}. \tag{11}$$

here $\mathbf{1}$ is a column vector whose entries are all ones, i.e.,

$$\mathbf{1} = \begin{bmatrix} 1 \\ \vdots \\ 1 \end{bmatrix},$$

Define the initial probability vector for the m_i transient states as

$$\boldsymbol{\alpha}_i = [\alpha_{i,1}, \cdots, \alpha_{i,m_i}], \quad i = h, r, c,$$

where $\alpha_{i,j}$ represents the initial probability at state j of process i, $i = h, r, c$, $j = 1, \ldots, m_i$. Then the probability of the absorbing state will be

$$\alpha_{i,m_i+1} = 1 - \boldsymbol{\alpha}_i \mathbf{1}.$$

Remark 3 When $m_i = 1$, the exponential distribution is obtained. Then subscript "1" can be dropped from $\lambda_{i,1}$ so that $\boldsymbol{B}_i = -\lambda_i$ is used in Section 3.1. □

The flow time to finish each process, t_i, $i = h, r, c$, i.e., the time to reach the absorbing state $m_i + 1$, is represented by a phase-type distribution. From (1), the total time t also follows a phase-type distribution. Then, based on the assumptions and definitions introduced in Section 2, the system performance measures, T, CV, and $S(T_d)$ can be evaluated.

Analogously to the exponential case, first, we derive the CDF of flow time, or the service rate of the system, under phase-type distribution assumption.

Theorem 2 *Under assumptions (i)-(v), the service rate for a given T_d, i.e., the CDF of system flow time, can be calculated as*

$$S(T_d) = P(t \leq T_d) = 1 - \boldsymbol{\alpha} e^{\boldsymbol{B}T_d} \mathbf{1}, \tag{12}$$

where $\boldsymbol{B}$ is a square matrix with dimension m, and $\boldsymbol{\alpha}$ is a row vector, which are defined as follows:

$$m = m_h m_r + m_h + m_r + m_c, \tag{13}$$

$$\boldsymbol{\alpha} = \begin{bmatrix} \boldsymbol{\alpha}_r \otimes \boldsymbol{\alpha}_h & \boldsymbol{\alpha}_r \alpha_{h,m_i+1} & \boldsymbol{\alpha}_h \alpha_{r,m_i+1} & \rho \boldsymbol{\alpha}_c \end{bmatrix}, \tag{14}$$

$$\boldsymbol{B} = \begin{bmatrix} \boldsymbol{B}_h \oplus \boldsymbol{B}_r & \boldsymbol{I}_h \otimes \boldsymbol{b}_r & \boldsymbol{b}_h \otimes \boldsymbol{I}_r & \mathbf{0} \\ \mathbf{0} & \boldsymbol{B}_h & \mathbf{0} & \boldsymbol{b}_h \boldsymbol{\alpha}_c \\ \mathbf{0} & \mathbf{0} & \boldsymbol{B}_r & \boldsymbol{b}_r \boldsymbol{\alpha}_c \\ \mathbf{0} & \mathbf{0} & \mathbf{0} & \boldsymbol{B}_c \end{bmatrix}, \tag{15}$$

and $\boldsymbol{b}_r$ and $\boldsymbol{b}_h$ are column vectors

$$\rho = 1 - \begin{bmatrix} \boldsymbol{\alpha}_r \otimes \boldsymbol{\alpha}_h & \boldsymbol{\alpha}_r \alpha_{h,m_h+1} & \boldsymbol{\alpha}_h \alpha_{r,m_r+1} \end{bmatrix} \mathbf{1}, \tag{16}$$

$$\boldsymbol{b}_i = \begin{bmatrix} 0 \\ \vdots \\ \lambda_{i,m_i} \end{bmatrix}, \quad i = r, h. \tag{17}$$

Proof: See Appendix A. ■

Remark 4 Note that $\otimes$ represents the Kronecker product, whose formula is provided in Appendix C. □

Remark 5 For exponential model, $m_i = 1$, $\boldsymbol{B}_i = -\lambda_i$, and $\boldsymbol{\alpha}_i = 1$, we obtain

$$\boldsymbol{B} = \begin{bmatrix} -\lambda_h - \lambda_r & \lambda_r & \lambda_h & 0 \\ 0 & -\lambda_h & 0 & \lambda_h \\ 0 & 0 & -\lambda_r & \lambda_r \\ 0 & 0 & 0 & -\lambda_c \end{bmatrix},$$

and

$$\boldsymbol{B}^{-1} = \begin{bmatrix} -\frac{1}{\lambda_h+\lambda_r} & -\frac{\lambda_r}{\lambda_h(\lambda_h+\lambda_r)} & -\frac{\lambda_h}{\lambda_r(\lambda_h+\lambda_r)} & -\frac{1}{\lambda_c} \\ 0 & -\frac{1}{\lambda_h} & 0 & -\frac{1}{\lambda_c} \\ 0 & 0 & -\frac{1}{\lambda_r} & -\frac{1}{\lambda_c} \\ 0 & 0 & 0 & -\frac{1}{\lambda_c} \end{bmatrix}.$$

It can be shown that the expressions derived in this subsection are equivalent to those obtained in Subsection 3.1. □

Using this result, for the average flow time of the system, we obtain

Corollary 3 *Under assumptions (i)-(v), the expected flow time of the system can be calculated as*

$$T = E(t) = -\boldsymbol{\alpha}\boldsymbol{B}^{-1}\mathbf{1}, \tag{18}$$

where $\boldsymbol{\alpha}$ and $\boldsymbol{B}$ are defined in (14).

Proof: See Appendix A. ■

For the CV of total flow time, we have

Corollary 4 *Under assumptions (i)-(v), the coefficient of variation of system flow time can be calculated as*

$$CV = \frac{\sqrt{2\boldsymbol{\alpha}\boldsymbol{B}^{-2}\mathbf{1} - \left(\boldsymbol{\alpha}\boldsymbol{B}^{-1}\mathbf{1}\right)^2}}{-\boldsymbol{\alpha}\boldsymbol{B}^{-1}\mathbf{1}}, \tag{19}$$

where $\boldsymbol{\alpha}$ and $\boldsymbol{B}$ are defined in (14)-(17) .

Proof: See Appendix A. ■

Remark 6 The above model can be extended to the scenarios where more than one robots and/or more than one operators collaborate in the system. For example, two or three operators may collaborate to install the front panel in a vehicle in the assembly line. In this case, the derived approach is still applicable. Assume there are k_r robots and k_h operators who will carry out their individual work first, then collaborate to finish the assembly. Then the system flow time can be characterized as

$$t = \max(t_{r,1} \ldots, t_{r,k_r}, t_{h,1}, \ldots, t_{h,k_h}) + t_c.$$

By applying the maximum function of two individual processes, we obtain a new process still following phase-type distribution. Then such a process is compared to the next individual process to obtain the maximums. Continue this procedure until the last individual process. Finally we can obtain the maximal work time of all independent processes. Then this time is summed up with the task time in the collaboration process, the overall flow time performance can be obtained. □

4 System Properties

4.1 Exponential Distribution Models

4.1.1 Monotonicity

Using the formulas introduced above, we investigate system properties. First, the exponential models are analyzed. By examining the expected flow time under exponential assumption, we observe monotonic properties with respect to its parameters. Such properties provide the foundation for work allocation and bottleneck analysis. Specifically, we expect that by reducing the work time of each step, the overall flow time will decrease.

Proposition 1 *Under assumptions (i)-(v) with 1 phase, i.e., $m_r = m_h = m_c = 1$, the expected flow time of the system is monotonically decreasing with respect to λ_r, λ_h, and λ_c.*

Proof: See Appendix B. ■

Similar monotonic properties exist for the CV of flow time.

Proposition 2 *Under assumptions (i)-(v) with 1 phase, i.e., $m_r = m_h = m_c = 1$, the CV of system flow time is monotonically decreasing with respect to λ_r, λ_h, and λ_c.*

Proof: See Appendix B. ■

4.1.2 Work allocation

In addition, if the total time to finish all the preparation tasks is a constant, what will be an optimal allocation of tasks to the operator and the cobot? To answer this question, we derive the following:

Proposition 3 *Under assumptions (i)-(v) with 1 phase, i.e., $m_r = m_h = m_c = 1$, given the constraint*

$$\frac{1}{\lambda_r} + \frac{1}{\lambda_h} = T_{prep} \tag{20}$$

where T_{prep} is the total work time of preparation tasks, then the system flow time is minimized if

$$\lambda_r = \lambda_h. \tag{21}$$

Proof: See Appendix B. ■

This result indicates that to effectively assign tasks, the operator and the cobot should be allocated the same amount of preparatory work (in terms of task time) so that they will have the same impact to the joint process.

4.1.3 Bottleneck analysis

In addition, when continuous improvement effort is contributed to the preparatory work, the step that can lead to a larger decrease in total flow time becomes the bottleneck and should be mitigated. It turns out the step with longer task time should be focused on, decreasing whose task time can result in more reduction in total flow time. Thus, we define

Definition 1 *Under assumptions (i)-(v) with 1 phase, i.e., $m_r = m_h = m_c = 1$, process i becomes the bottleneck if $\forall i, k \in \{h, r, c\}$,*

$$\Big|\frac{\partial T}{\partial \lambda_i}\Big| \geq \Big|\frac{\partial T}{\partial \lambda_k}\Big|, \quad k \neq i. \tag{22}$$

Under definition 1, to identify a bottleneck, we first focus on the preparation processes.

Proposition 4 *Under assumptions (i)-(v) with 1 phase, i.e., $m_r = m_h = m_c = 1$, then $\forall i, k \in \{h, r\}$,*

$$\Big|\frac{\partial T}{\partial \lambda_i}\Big| \geq \Big|\frac{\partial T}{\partial \lambda_k}\Big| \text{ if and only if } \lambda_i \leq \lambda_k. \tag{23}$$

Proof: See Appendix B. ■

Using this result, a bottleneck indicator can be obtained:

Bottleneck Indicator 1: In the collaborative assembly system with exponential process times, among the preparation processes, the one takes longer time is the bottleneck.

Next we investigate the bottleneck of all processes. Comparing changes in λ_c and λ_r or λ_h, the following is obtained:

Proposition 5 *Under assumptions (i)-(v) with 1 phase, i.e., $m_r = m_h = m_c = 1$, then $\forall k \in \{h, r\}$,*

$$\left|\frac{\partial T}{\partial \lambda_k}\right| \geq \left|\frac{\partial T}{\partial \lambda_c}\right| \text{ if and only if } \frac{1}{\lambda_k^2} \geq \frac{1}{(\lambda_h + \lambda_r)^2} + \frac{1}{\lambda_c^2}. \tag{24}$$

Proof: See Appendix B. ∎

Proposition 5 implies that if the square of a preparation process's time is larger than the sum of square of collaboration process time and square of "combined" or "overlapped" time (see the explanation after Corollary 1 in Section 3.1). In other words, only when the preparation time is significantly longer than the collaboration time, then the longer preparation process will become the bottleneck.

To find the bottleneck of the whole system, Bottleneck Indicator 1 can be used first to find the longer preparation process and then to compare with the collaboration process using Proposition 5 to determine the system bottleneck.

Bottleneck Indicator 2: In the collaborative assembly system with exponential process times, the longer preparation processes is bottleneck if its time is substantially longer than the collaboration time (i.e., using Proposition 5), otherwise the collaboration process is the bottleneck.

4.2 Phase-type Distribution Models

4.2.1 Monotonicity

When each process consists of more than one sub-processes, the phase-type distribution with multiple phases will be used. As we expected, the monotonic properties with respect to collaboration process task times derived in the exponential cases still hold. In other words, reducing any collaboration sub-process task time (i.e., increasing task rate), the overall flow time will be decreased.

Proposition 6 *Under assumptions (i)-(v), the expected flow time of the system is monotonically decreasing with respect to λ_{cj}, $j = 1, \ldots, m_c$.*

Proof: See Appendix B. ∎

The monotonicity with respect to task times in operator and robot preparation processes also holds. Analytical proofs for the case of smaller number of phases, such as $m_h, m_r \leq 4$, can be obtained. However, for processes with more phases, the expression of partial derivatives of complex matrices becomes difficult to obtain, which makes the derivation of closed form result all but impossible. Note that although an explicit expression of partial derivatives with respect to T may not be available for all cases, numerical calculation of the derivatives can always be carried out. Thus, based on extensive numerical experiments by testing various randomly generated parameters, we formulate the result as a numerical fact.

Numerical Fact 1 *Under assumptions (i)-(v), the expected flow time of the system is monotonically decreasing with respect to λ_{ij}, $i = h, r$, and $j = 1, \ldots, m_i$.*

An illustration of monotonic property with respect to $\lambda_{h,j}$ is provided in Figure 3, where parameters B_h, B_r, and B_c are defined below.

$$\begin{aligned}
\boldsymbol{B}_h &= \begin{bmatrix} -\lambda_{h,1} & \lambda_{h,1} & 0 & 0 & 0 \\ 0 & -0.2 & 0.2 & 0 & 0 \\ 0 & 0 & -\lambda_{h,3} & \lambda_{h,3} & 0 \\ 0 & 0 & 0 & -0.43 & 0.43 \\ 0 & 0 & 0 & 0 & -\lambda_{h,5} \end{bmatrix}, \\
\boldsymbol{B}_r &= \begin{bmatrix} -0.1 & 0.1 & 0 & 0 \\ 0 & -0.25 & 0.25 & 0 \\ 0 & 0 & -0.32 & 0.32 \\ 0 & 0 & 0 & -0.66 \end{bmatrix}, \\
\boldsymbol{B}_c &= -1,
\end{aligned} \tag{25}$$

where the base values of $\lambda_{h,1}$, $\lambda_{h,3}$, and $\lambda_{h,5}$ are 0.1, 0.34, and 0.55, respectively. By varying one $\lambda_{h,i}$, $i = 1, 3, 5$, each time, we obtain the corresponding curve of flow time, showing as the red solid line, black dashed line, and green dotted line in Figure 3. As we can observe, all of them indicate decreasing patterns.

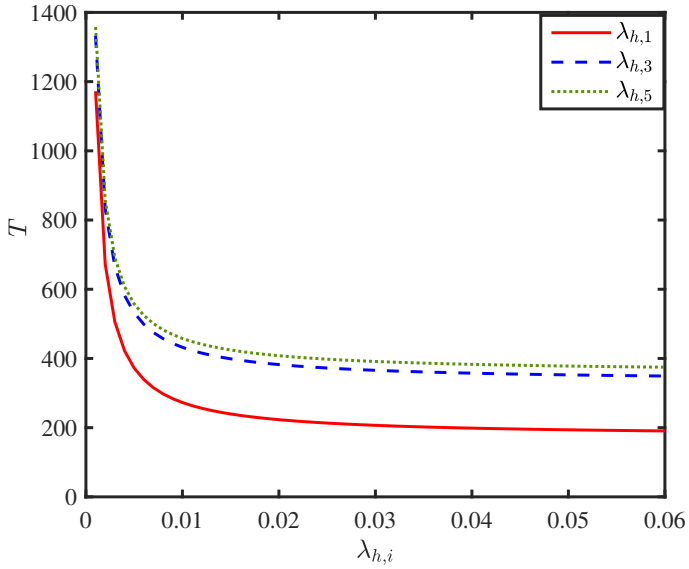

Figure 3: Monotonicity

4.2.2 Work allocation

Concerning about task allocation, again when the preparation processes and tasks are symmetrically assigned, i.e., well balanced, then the overall flow time is minimized.

Proposition 7 *Under assumptions (i)-(v), given the constraint*

$$\sum_{j=1}^{m_r} \frac{1}{\lambda_{r,j}} + \sum_{j=1}^{m_h} \frac{1}{\lambda_{h,j}} = T_{prep}, \tag{26}$$

where T_{prep} is the total work time of preparation tasks, then the system flow time is minimized if

$$m_r = m_h, \qquad \lambda_{r,j} = \lambda_{h,j}, \quad j = 1, \ldots, m_r. \tag{27}$$

Proof: See Appendix B. ∎

4.2.3 Bottleneck analysis

To identify a bottleneck in a phase-type distribution model, first, we consider the preparation process and the collaboration process individually.

Definition 2 *Under assumptions (i)-(v), sub-process j becomes the bottleneck of process i if $\forall i \in \{h, r, c\}$ and $k, j \in \{1, \ldots, m_i\}$,*

$$\left|\frac{\partial T}{\partial \lambda_{i,j}}\right| \geq \left|\frac{\partial T}{\partial \lambda_{i,k}}\right|, \quad k \neq j. \tag{28}$$

Under definition 2, in each processes, the step with the longest task time becomes the bottleneck in the corresponding process. Improving such a task time can lead to larger improvement in system flow time comparing with improving other step's task times. To investigate this, we first focus on the collaboration process.

Proposition 8 *Under assumptions (i)-(v), $\forall k \neq j$ and $k, j \in \{1, \ldots, m_c\}$,*

$$\Big|\frac{\partial T}{\partial \lambda_{c,j}}\Big| \geq \Big|\frac{\partial T}{\partial \lambda_{c,k}}\Big|, \text{ if and only if } \lambda_{c,j} \leq \lambda_{c,k}. \tag{29}$$

Proof: See Appendix B. ∎

Next, for the human and robot preparation processes, this property still holds, however, a rigorous proof is not available due to lack of closed form analytical expressions. Thus, we again formulate it as a numerical fact after extensive experiments.

Numerical Fact 2 *Under assumptions (i)-(v), $\forall i \in \{r, h\}$, $k \neq j$, and $k, j \in \{1, \ldots, m_i\}$,*

$$\Big|\frac{\partial T}{\partial \lambda_{i,j}}\Big| \geq \Big|\frac{\partial T}{\partial \lambda_{i,k}}\Big| \text{ if and only if } \lambda_{i,j} \leq \lambda_{i,k}. \tag{30}$$

To present an example of this fact, we consider the parameters shown in (25), and compare $\lambda_{h,1}$ and $\lambda_{h,3}$ under various values. As we can see from the results in Table 1, when $\lambda_{h,1} > \lambda_{h,3}$, we always obtain $\Big|\frac{\partial T}{\partial \lambda_{h,1}}\Big| > \Big|\frac{\partial T}{\partial \lambda_{h,3}}\Big|$.

Table 1: Example of Numerical Fact 2

$\Big\lvert\frac{\partial T}{\partial \lambda_{h,1}}\Big\rvert - \Big\lvert\frac{\partial T}{\partial \lambda_{h,3}}\Big\rvert$		$\lambda_{h,1}$				
		0.05	0.10	0.15	0.20	0.25
$\lambda_{h,3}$	0.05	0	-283.13	-329.87	-343.99	-349.46
	0.10	283.13	0	-47.29	-62.00	-68.00
	0.15	329.87	47.29	0	-14.85	-21.01
	0.20	343.99	62.00	14.86	0	-6.20
	0.25	349.46	68.00	21.01	6.20	0

The above results indicate that, to identify the bottleneck, we can only compare the impact of improvement on the step with the longest task time in each process. Thus, the following bottleneck indicator is obtained:

Bottleneck Indicator 3: In the collaborative assembly system with phase-type process times, the step with the longest task time in each processes is the bottleneck of the corresponding process.

The bottleneck of the whole system is the step who can lead to the largest improvement of overall flow time. Thus, we define

Definition 3 *Under assumptions (i)-(v), $\forall (k, l) \neq (i, j)$,*

$$\Big|\frac{\partial T}{\partial \lambda_{i,j}}\Big| \geq \Big|\frac{\partial T}{\partial \lambda_{k,l}}\Big|, \quad i, k, \in \{h, r, c\}, j \in \{1, \ldots, m_i\}, l \in \{1, \ldots, m_k\}. \tag{31}$$

Under Definition 3, using Proposition 8 and Numerical Fact 2, the system bottleneck must be among the three bottlenecks identified in each process. Then, using equation (31), the largest partial derivative can be selected from these three bottlenecks.

4.3 Comparisons

In addition, it is of interest to compare the models with exponential process time (Section 3.1) and phase-type process time (Section 3.2). Through extensive numerical experiments, we obtain

Numerical Fact 3 *Under assumptions (i)-(v), if*

$$\frac{1}{\lambda_i^{\exp}} = \sum_{j=1}^{m_i} \frac{1}{\lambda_{i,j}^{\mathrm{PH}}}, \quad i = h, r, c, \tag{32}$$

then

$$T^{\text{exp}} \geq T^{\text{PH}}, \quad CV^{\text{exp}} \geq CV^{\text{PH}}, \tag{33}$$

where superscripts "exp" and "PH" indicate the parameters and performance measures for exponential and phase-type models, respectively.

An illustration of the numerical fact is presented in Figure 4 for both T and CV, where parameter $\lambda_h^{\text{exp}} = 0.001$ in the exponential model, and the parameters in the phase-type model are from (25). To ensure the overall task time of human preparation process will be the same in both models, we set constraint

$$\sum_{i=1}^{5} \frac{1}{\lambda_{h,i}^{\text{PH}}} = \frac{1}{\lambda_h^{\text{exp}}}. \tag{34}$$

When $\lambda_{h,4}^{\text{PH}} = 0.02$, $\lambda_{h,5}^{\text{PH}} = 0.07$, we vary $\lambda_{h,1}^{\text{PH}}$ and $\lambda_{h,2}^{\text{PH}}$. Then $\lambda_{h,3}^{\text{PH}}$ will be determined due to constraint (34). As one can see from Figure 4, the resulting differences, $T^{\text{exp}} - T^{\text{PH}}$ in expected flow time and $CV^{\text{exp}} - CV^{\text{PH}}$ in CV, are all positive, which imply that the exponential model always provides higher values.

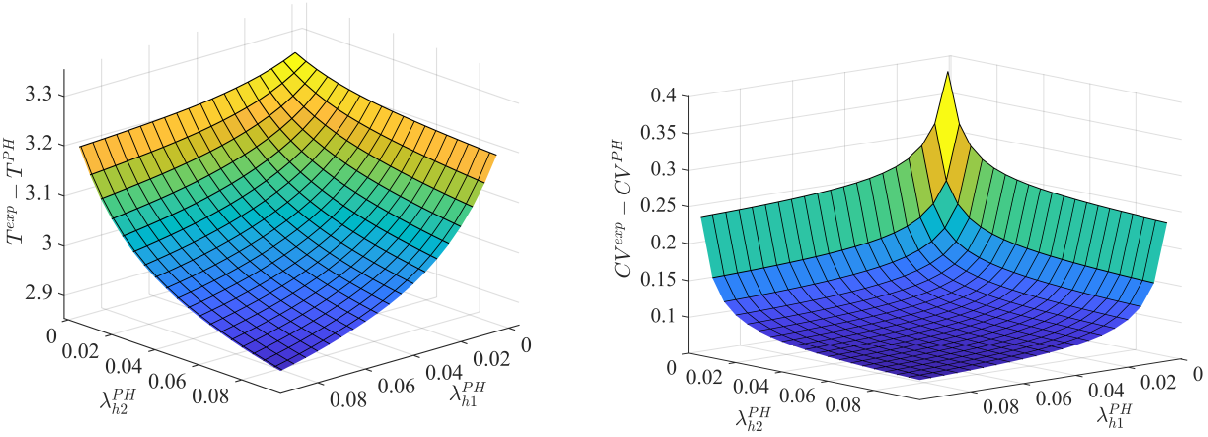

(a) Comparison of expected flow time

(b) Comparison of CV

Figure 4: Comparisons between exponential and phase-type models

When more than 1 phases are included in each process (note that exponential model can be viewed as a phase-type model with only 1 phase), the process variability will be decreased, which will lead to smaller T and CV. This result indicates that when exponential model is used for performance evaluation, we may obtain the upper bounds (in terms of flow time and its variability) or lower bounds (in terms of throughput), which can be a good reference in designing the collaborative assembly processes.

5 Case Study

To illustrate the applicability of the model and method, a case study at a front panel assembly station in an automotive assembly plant is carried out.

5.1 System Description and Modeling

The following processes are conducted in the assembly station: The cobot moves automatically to the rack, picks up the panel, and transports the panel close to the car body on a moving line. While the cobot is transporting the panel, one operator prepares the necessary fitting in the car body. Then this operator holds the cobot to guide the panel into car body and set unto the right location, and the second operator secures

the panel. Afterwards, the cobot is returning to the rack, while the first operator moves to the next vehicle to start preparation, and the second operator continues finishing the assembly tasks on the current vehicle. A graphical illustration of such an assembly station is presented in Figure 5, where the dashed lines represent the movement paths of the cobot and the operator.

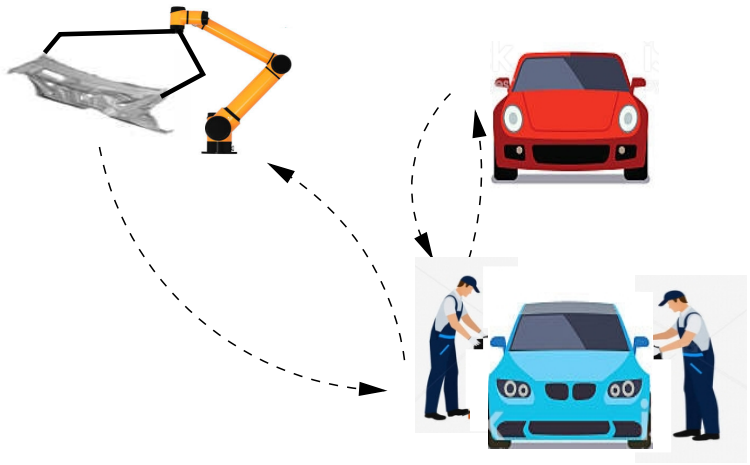

Figure 5: Panel assembly system model

To model such a collaborative assembly system, we characterize the activities into the following steps in each process, shown in Figure 6, where λ_{ij} represents the parameter of each step and i and j indicates the process ID and step number, respectively.

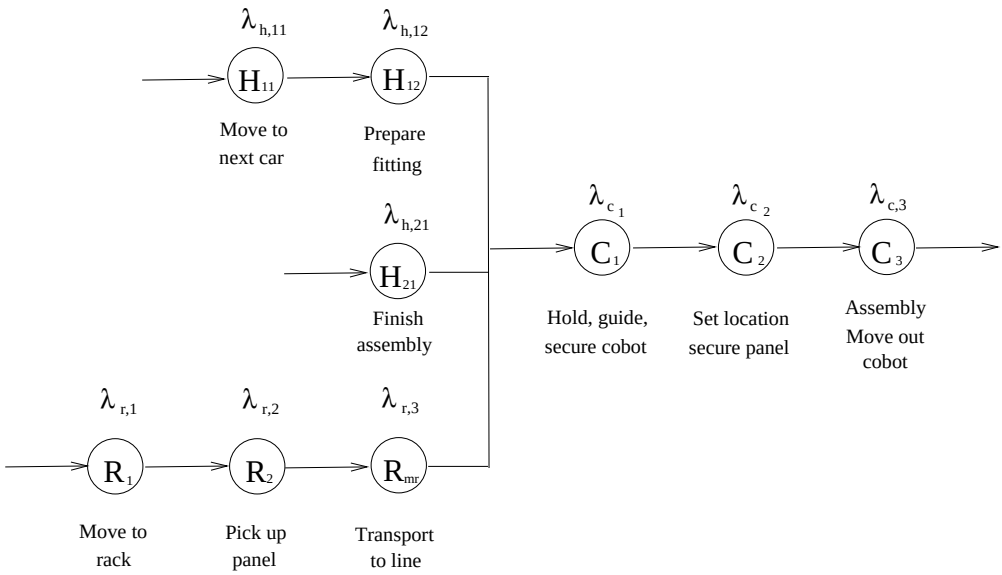

Figure 6: Panel assembly system model

- Robot: The robot moves automatically to the rack; picks up the panel; and transports the panel close to the vehicle body on a moving assembly line.
- Human operators: When robot is moving to the rack and transporting the panel, Operator 1 starts to prepare the necessary fitting inside the current vehicle, and Operator 2 is finishing the assembly of previous vehicle.

- Collaboration: Operator 1 holds the robot to guide the panel into the vehicle body and set onto the right location, and Operator 2 secures the panel and start assembly. Then Operator 1 moves the robot out of the vehicle.

Note that although the second operator is working on the previous vehicle while the first operator and cobot start preparing for the current one, we still count the work of the second operator as a "preparation" one since the operator can only start working on the current vehicle afterwards. In addition, these two operators work on the two sides of the vehicle. Through observations of the operations, time stamps are recorded and the task times are evaluated and shown in Table 2 (note that due to confidentially reason, the data has been modified and is used for illustration only). By taking the inverse of task times, λ_{ij}'s are obtained.

Table 2: Task description and work time (sec)

Robot	R_1:	Move to rack automatically	10.1	$\lambda_{r,1}: 0.099$
	R_2:	Pick up panel	12.1	$\lambda_{r,2}: 0.0826$
	R_3:	Transport panel to the line	2.5	$\lambda_{r,3}: 0.4$
Human	H_{11} (Operator 1):	Walk to the next car	9	$\lambda_{h,11}: 0.1111$
	H_{12} (Operator 1):	Prepare fitting	15.5	$\lambda_{h,12}: 0.0645$
	H_{21} (Operator 2):	Finish assembly of the previous car	30	$\lambda_{h,21}: 0.0333$
Collaboration	C_1:	Hold, guide, and secure cobot	8.2	$\lambda_{c,1}: 0.1220$
	C_2:	Set location and secure panel	8.2	$\lambda_{c,2}: 0.1220$
	C_3:	Assembly and move out cobot	4.5	$\lambda_{c,3}: 0.2222$

5.2 Performance Analysis

Using these parameters, we consider the individual processes of the operators and the cobot, i.e., H_1, H_2, and R, with task times t_{h_1}, t_{h_2}, and t_r, respectively. Introduce process H with $t_h = \max(t_{h_1}, t_{h_2})$. Then the system flow time can be defined as

$$t = \max(t_h, t_r) + t_c = \max(\max(t_{h_1}, t_{h_2}), t_r) + t_c,$$

where

$$\begin{aligned}
&m_{h_1} = 2, \quad m_{h_2} = 1, \quad m_r = 3, \quad m_c = 3,\\
&\boldsymbol{\alpha}_{h_1} = [1, 0], \quad \alpha_{h_2} = 1, \quad \boldsymbol{\alpha}_r = \boldsymbol{\alpha}_c = [1, 0, 0],\\
&\boldsymbol{B}_{h_1} = \begin{bmatrix} -\lambda_{h,11} & \lambda_{h,11} \\ 0 & -\lambda_{h,12} \end{bmatrix}, \quad \boldsymbol{B}_{h_2} = -\lambda_{h,21},\\
&\boldsymbol{B}_r = \begin{bmatrix} -\lambda_{r,1} & \lambda_{r,1} & 0 \\ 0 & -\lambda_{r,2} & \lambda_{r,2} \\ 0 & 0 & -\lambda_{r,3} \end{bmatrix}, \quad \boldsymbol{B}_c = \begin{bmatrix} -\lambda_{c,1} & \lambda_{c,1} & 0 \\ 0 & -\lambda_{c,2} & \lambda_{c,2} \\ 0 & 0 & -\lambda_{c,3} \end{bmatrix}.
\end{aligned}$$

To evaluate the system performance, first, we obtain parameters m_h, $\boldsymbol{\alpha}_h$, $\boldsymbol{B}_h$ for process H using $H = \max(H_1, H_2)$. From the proof of Theorem 2, we have

$$\begin{aligned}
&m_h = m_{h_1} m_{h_2} + m_{h_1} + m_{h_2} = 5, \quad \boldsymbol{\alpha}_h = [1, 0, 0, 0, 0],\\
&\boldsymbol{B}_h = \begin{bmatrix} \lambda_{h,11}\lambda_{h,21} & -\lambda_{h,11}\lambda_{h,21} & \lambda_{h,21} & 0 & 0 \\ 0 & \lambda_{h,12}\lambda_{h,21} & 0 & \lambda_{h,21} & \lambda_{h,12} \\ 0 & 0 & -\lambda_{h,11} & \lambda_{h,11} & 0 \\ 0 & 0 & 0 & -\lambda_{h,12} & 0 \\ 0 & 0 & 0 & 0 & -\lambda_{h,21} \end{bmatrix}.
\end{aligned}$$

Solving $\boldsymbol{B}$ and $\boldsymbol{\alpha}$, and considering processes of operators (H), robot (R), and collaboration (C), from Corollaries 3 and 4, the mean and CV of flow time for the panel assembly process can be calculated.

$$T^{\mathrm{PH}} = 65.8869, \qquad CV^{\mathrm{PH}} = 0.4452.$$

Similarly, for a given T_d, service rate $S^{\text{PH}}(T_d)$ can be derived as shown in (35).

$$\begin{aligned}S^{\text{PH}}(T_d) = {} & 0.0206e^{-\frac{2T_d}{5}} + 346.3643e^{-\frac{21T_d}{100}} - 123.6768e^{-\frac{18T_d}{125}} - 0.0070e^{-\frac{68T_d}{125}} - 15.6311e^{-\frac{13T_d}{200}} \\ & + 6760.5217e^{-\frac{29T_d}{250}} - 2530.9393e^{-\frac{33T_d}{250}} + 1244.44386e^{-\frac{37T_d}{250}} - 537.2332e^{-\frac{41T_d}{250}} \\ & - 0.0240e^{-\frac{93T_d}{200}} + 111.6333e^{-\frac{49T_d}{500}} - 5359e^{-\frac{61T_d}{500}} - 251.1430e^{-\frac{97T_d}{500}} + 382.0859e^{-\frac{111T_d}{500}} \\ & + 0.0176e^{-\frac{249T_d}{500}} - 2.2071e^{-\frac{33T_d}{1000}} - 122.0238e^{-\frac{83T_d}{1000}} + 350.0769e^{-\frac{99T_d}{1000}} + 347.6321e^{-\frac{111T_d}{1000}} \\ & - 436.1801e^{-\frac{181T_d}{1000}} + 390.8651e^{-\frac{197T_d}{1000}} - 661.2954e^{-\frac{227T_d}{1000}} + 104.6863e^{-\frac{243T_d}{1000}} - 0.0139e^{-\frac{433T_d}{1000}} \\ & + 0.0092e^{-\frac{511T_d}{1000}} - 70.2142te^{-\frac{61T_d}{500}} + 1. \end{aligned} \tag{35}$$

To compare with the exponential distribution model, we also obtain the performance measure under 1 phase task time for each process,

$$T^{\text{exp}} = 69.5674, \qquad CV^{\text{exp}} = 0.5414.$$

For a given T_d, service rate $S^{\text{exp}}(T_d)$ is shown in (36).

$$\begin{aligned}S^{\text{exp}}(T_d) = {} & 0.7166e^{-\frac{229T_d}{2000}} - 6.8286e^{-\frac{51T_d}{1250}} - 6.4595e^{-\frac{101T_d}{2500}} - 1.4311e^{-\frac{203T_d}{2500}} + 19.9621e^{-\frac{239T_d}{5000}} \\ & - 3.2966e^{-\frac{333T_d}{10000}} - 1.8456e^{-\frac{737T_d}{10000}} - 1.8175e^{-\frac{741T_d}{10000}} + 1. \end{aligned} \tag{36}$$

Both results are verified through simulation experiments. As we can see, the mean flow time and CV in the exponential model are both higher than those in the phase-type model. This is also visible from the flow time distributions. From the derived service rates (see equations (35) and (36)), we can derive the complete distributions of system flow time, shown in Figures 7(a) and (b) for cumulative distribution function (S) and probability density function (s), respectively. The flow times of phase-type and exponential distribution models are depicted by red dashed line and blue solid line, respectively, in both figures. These figures indicate that the exponential model has a higher variability, which is due to higher CV in each process. Particularly, the service rate becomes lower in exponential model when T_d becomes longer. Such results also verify Numerical Fact 3 in Subsection 4.3.

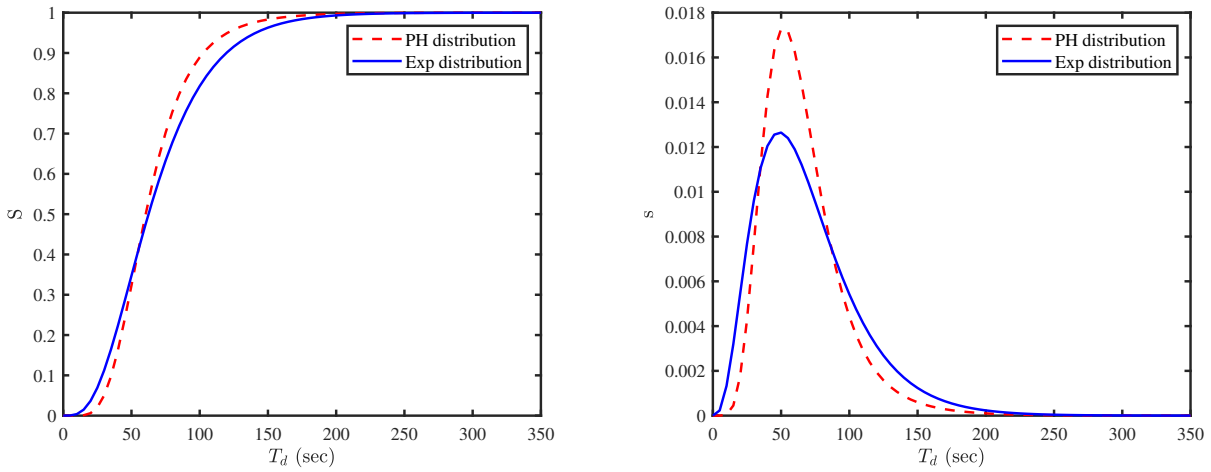

(a) CDF (b) PDF

Figure 7: CDF and PDF of system flow time

5.3 Continuous Improvement

To improve the system performance by reducing system flow time, bottleneck analysis is carried out to seek the largest potential improvement of the process.

Using Bottleneck Indicator 3, we identify steps R_2 and H_{12} as the bottlenecks in robot and Operator 1 processes, respectively. As C_1 or C_2 have the same task time, they both are bottlenecks in the collaboration process. Operator 2 only has one process, thus H_{21} is the only choice. In addition, we observe that Operator 2 (H_{21}) has a much longer process than any other ones. Thus, it becomes the bottleneck of the whole system. This can also be verified by calculating the partial derivatives. By speeding up to reduce Operator 2's task time or allocating part of the Operator 2's task to Operator 1 or the collaboration process, the overall flow time can be decreased. The feasibility of potential time reduction or task redistribution in practice is under investigation.

6 Conclusions

Collaborative robots are becoming more and more popular in many manufacturing industries. Effective modeling and analysis of assembly systems with collaborative robots are necessary and important. In this paper, a system-theoretic method is proposed to evaluate the flow time performance of collaborative assembly systems. Analytical formulas for expected flow time and its variation, as well as the service rate are derived under both exponential and phase-type distributions of process times. The system properties are investigated and bottleneck analyses are carried out. A case study at an automotive front panel assembly station is presented to illustrate the applicability of the method.

To extend this work, the following directions can be considered:

- developing methods for multi-stage collaborative assembly processes, where each stage can be either robotic, manual, or collaboration operations. A possible approach is to derive the performance for a two-stage system first, and then extend to multiple stages.
- including not only flow time but also ergonomic and safety measurements in the model, e.g., to also evaluate stress and fatigue indices in each process. The challenge lies in how to integrate the time and ergonomic measurements into one performance index.
- considering cognitive issues in human cobot collaboration activities, which can affect both time and ergonomic performances.
- extending to other random process models, and particularly, including possible robot breakdowns;
- investigating the possibility of real-time reallocation of tasks to minimize waiting times, such as starting joint work earlier when human preparation finishes first;
- introducing multi-objective optimization models for system design to optimally assign tasks to human operator and cobots to minimize flow time and reduce fatigue and injuries, and
- finally, applying models on the factory floor to improve both productivity and ergonomic performances.

The development of such methods will provide quantitative tools for production engineers and managers to design and evaluate tasks in collaborative systems to improve productivity, safety and ergonomics.

Appendix A: Proofs for Section 3.1

Proof of Theorem 1: The service rate can be calculated as

$$\begin{aligned}
S(T_d) = P(t \le T_d) &= \int_0^{T_d} P(\max(t_r, t_h) + t_c \le T_d | t_c) f_{t_c} dt_c = \int_0^{T_d} P(\max(t_r, t_h) \le T_d - t_c) \lambda_c e^{-\lambda_c t_c} dt_c \\
&= \int_0^{T_d} P(t_r \le T_d - t_c, t_h \le T_d - t_c) \lambda_c e^{-\lambda_c t_c} dt_c = \int_0^{T_d} P(t_r \le T_d - t_c) P(t_h \le T_d - t_c) \lambda_c e^{-\lambda_c t_c} dt_c \\
&= \int_0^{T_d} [1 - e^{-\lambda_r (T_d - t_c)}][1 - e^{-\lambda_h (T_d - t_c)}] \lambda_c e^{-\lambda_c t_c} dt_c \\
&= \int_0^{T_d} [\lambda_c e^{-\lambda_c t_c} - e^{-\lambda_r (T_d - t_c)} \lambda_c e^{-\lambda_c t_c} - e^{-\lambda_h (T_d - t_c)} \lambda_c e^{-\lambda_c t_c} + \lambda_c e^{-\lambda_r (T_d - t_c)} e^{-\lambda_h (T_d - t_c)} e^{-\lambda_c t_c}] dt_c
\end{aligned}$$

$$= \int_0^{T_d} [\lambda_c e^{-\lambda_c t_c} - \lambda_c e^{-(\lambda_c t_c + \lambda_r (T_d - t_c))} - \lambda_c e^{-(\lambda_c t_c + \lambda_h (T_d - t_c))} + \lambda_c e^{-(\lambda_r (T_d - t_c) + \lambda_h (T_d - t_c) + \lambda_c t_c)}] dt_c$$
$$= \int_0^{T_d} [\lambda_c e^{-\lambda_c t_c} - \lambda_c e^{-\lambda_r T_d} e^{-(\lambda_c - \lambda_r) t_c} - \lambda_c e^{-\lambda_h T_d} e^{-(\lambda_c - \lambda_h) t_c} + \lambda_c e^{-(\lambda_r + \lambda_h) T_d} e^{-(\lambda_c - \lambda_r - \lambda_h) t_c}] dt_c.$$

If

$$\lambda_c \neq \lambda_h, \quad \lambda_c \neq \lambda_r, \quad \lambda_c \neq \lambda_h + \lambda_r, \tag{A.1}$$

it follows that

$$\begin{aligned} S(T_d) &= 1 - e^{-\lambda_c T_d} - \frac{\lambda_c e^{-\lambda_r T_d} (1 - e^{-(\lambda_c - \lambda_r) T_d})}{\lambda_c - \lambda_r} - \frac{\lambda_c e^{-\lambda_h T_d} (1 - e^{-(\lambda_c - \lambda_h) T_d})}{\lambda_c - \lambda_h} \\ &\quad + \frac{\lambda_c e^{-(\lambda_r + \lambda_h) T_d} (1 - e^{-(\lambda_c - \lambda_r - \lambda_h) T_d})}{\lambda_c - \lambda_r - \lambda_h} \\ &= 1 - e^{-\lambda_c T_d} - \frac{\lambda_c (e^{-\lambda_r T_d} - e^{-\lambda_c T_d})}{\lambda_c - \lambda_r} - \frac{\lambda_c (e^{-\lambda_h T_d} - e^{-\lambda_c T_d})}{\lambda_c - \lambda_h} + \frac{\lambda_c (e^{-(\lambda_r + \lambda_h) T_d} - e^{-\lambda_c T_d})}{\lambda_c - \lambda_r - \lambda_h}. \end{aligned}$$

If any inequality in (A.1) becomes an equality, the corresponding exponential power term in the integral equation above (A.1) can be simplified by zero. Then the integral can be derived immediately. Define γ_r, γ_h, and γ_{rh} as

$$\gamma_r = \begin{cases} \frac{e^{-\lambda_r T_d} - e^{-\lambda_c T_d}}{\lambda_c - \lambda_r}, & \text{if } \lambda_c \neq \lambda_r, \\ T_d e^{-\lambda_r T_d}, & \text{o/w}, \end{cases}$$
$$\gamma_h = \begin{cases} \frac{e^{-\lambda_h T_d} - e^{-\lambda_c T_d}}{\lambda_c - \lambda_h}, & \text{if } \lambda_c \neq \lambda_h, \\ T_d e^{-\lambda_h T_d}, & \text{o/w}, \end{cases}$$
$$\gamma_{rh} = \begin{cases} \frac{e^{-(\lambda_r + \lambda_h) T_d} - e^{-\lambda_c T_d}}{\lambda_c - \lambda_r - \lambda_h}, & \text{if } \lambda_c \neq \lambda_r + \lambda_h, \\ T_d e^{-(\lambda_r + \lambda_h) T_d}, & \text{o/w}. \end{cases}$$

Then, service rate S can be expressed by

$$S(T_d) = 1 - e^{-\lambda_c T_d} + \lambda_c (\gamma_{rh} - \gamma_r - \gamma_h),$$

■

Proof of Corollary 1: First, we calculate the probability density function $s(t)$.

$$s(t) = \lambda_c e^{-\lambda_c t} - \lambda_c \left(\frac{d\gamma_{rh}(t)}{dt} - \frac{d\gamma_r(t)}{dt} - \frac{d\gamma_h(t)}{dt} \right). \tag{A.2}$$

For the cases satisfying (A.1), we have

$$s(t) = \lambda_c e^{-\lambda_c t} - \frac{\lambda_c (-\lambda_r e^{-\lambda_r t} + \lambda_c e^{-\lambda_c t})}{\lambda_c - \lambda_r} - \frac{\lambda_c (-\lambda_h e^{-\lambda_h t} + \lambda_c e^{-\lambda_c t})}{\lambda_c - \lambda_h} + \frac{\lambda_c (-(\lambda_r + \lambda_h) e^{-(\lambda_r + \lambda_h) t} + \lambda_c e^{-\lambda_c t})}{\lambda_c - \lambda_r - \lambda_h}.$$

Then the expected time to finish the whole assembly process can be calculated as

$$\begin{aligned} T &= \int_0^\infty t s(t) dt = \int_0^\infty \Big(\lambda_c t e^{-\lambda_c t} - \frac{\lambda_c (-\lambda_r t e^{-\lambda_r t} + \lambda_c t e^{-\lambda_c t})}{\lambda_c - \lambda_r} - \frac{\lambda_c (-\lambda_h t e^{-\lambda_h t} + \lambda_c t e^{-\lambda_c t})}{\lambda_c - \lambda_h} \\ &\quad + \frac{\lambda_c (-(\lambda_r + \lambda_h) t e^{-(\lambda_r + \lambda_h) t} + \lambda_c t e^{-\lambda_c t})}{\lambda_c - \lambda_r - \lambda_h} \Big) dt \\ &= \frac{1}{\lambda_c} + \frac{\lambda_c}{\lambda_c - \lambda_r} \Big(\frac{1}{\lambda_r} - \frac{1}{\lambda_c} \Big) + \frac{\lambda_c}{\lambda_c - \lambda_h} \Big(\frac{1}{\lambda_h} - \frac{1}{\lambda_c} \Big) - \frac{\lambda_c}{\lambda_c - \lambda_r - \lambda_h} \Big(\frac{1}{\lambda_h + \lambda_r} - \frac{1}{\lambda_c} \Big) \\ &= \frac{1}{\lambda_c} + \frac{1}{\lambda_r} + \frac{1}{\lambda_h} - \frac{1}{\lambda_r + \lambda_h}. \end{aligned} \tag{A.3}$$

If any inequality in (A.1) becomes an equality, the derivative of terms γ_r, γ_h, or γ_{rh}, for the cases of $\lambda_c = \lambda_r$, $\lambda_c = \lambda_h$, or $\lambda_c = \lambda_r + \lambda_h$, respectively, can be derived as

$$\left.\frac{d\gamma_r(t)}{dt}\right|_{\lambda_c=\lambda_r} = \left.\frac{d\gamma_h(t)}{dt}\right|_{\lambda_c=\lambda_h} = \left.\frac{d\gamma_{rh}(t)}{dt}\right|_{\lambda_c=\lambda_h+\lambda_r} = \frac{dte^{-\lambda_c t}}{dt} = e^{-\lambda_c t}(1-\lambda_c t). \tag{A.4}$$

Then, with similar derivation to (A.3), we have

$$\begin{aligned}
-\lambda_c \int_0^\infty te^{-\lambda_c t}(1-\lambda_c t)dt &= -\lambda_c \int_0^\infty te^{-\lambda_c t}dt + \lambda_c \int_0^\infty \lambda_c t^2 e^{-\lambda_c t}dt \\
&= -\lambda_c \int_0^\infty te^{-\lambda_c t}dt + t^2 e^{-\lambda_c t}\Big|_0^\infty + \lambda_c \int_0^\infty e^{-\lambda_c t}dt^2 \\
&= \lambda_c \int_0^\infty te^{-\lambda_c t}dt = \frac{1}{\lambda_c},
\end{aligned}$$

Thus, when any inequality becomes an equality, i.e., either $\lambda_c = \lambda_h$, or $\lambda_c = \lambda_r$, or $\lambda_c = \lambda_h + \lambda_r$, equation (A.3) can be obtained as well. ∎

Proof of Corollary 2: From equation (A.2), first, we consider the cases satisfying (A.1), and derive $E(t^2)$.

$$\begin{aligned}
E(t^2) &= \int_0^\infty t^2 s(t)dt = \int_0^\infty \Big(\lambda_c t^2 e^{-\lambda_c t} - \frac{\lambda_c(-\lambda_r t^2 e^{-\lambda_r t} + \lambda_c t^2 e^{-\lambda_c t})}{\lambda_c - \lambda_r} - \frac{\lambda_c(-\lambda_h t^2 e^{-\lambda_h t} + \lambda_c t^2 e^{-\lambda_c t})}{\lambda_c - \lambda_h} \\
&\quad + \frac{\lambda_c(-(\lambda_r+\lambda_h)t^2 e^{-(\lambda_r+\lambda_h)t} + \lambda_c t^2 e^{-\lambda_c t})}{\lambda_c - \lambda_r - \lambda_h}\Big)dt \\
&= \int_0^\infty (-t^2)de^{-\lambda_c t} + \int_0^\infty \frac{\lambda_c(-t^2)}{\lambda_c - \lambda_r}de^{-\lambda_r t} - \int_0^\infty \frac{\lambda_c(-t^2)}{\lambda_c - \lambda_r}de^{-\lambda_c t} + \int_0^\infty \frac{\lambda_c(-t^2)}{\lambda_c - \lambda_h}de^{-\lambda_h t} \\
&\quad - \int_0^\infty \frac{\lambda_c(-t^2)}{\lambda_c - \lambda_h}de^{-\lambda_c t} + \int_0^\infty \frac{\lambda_c(-t^2)}{\lambda_c - \lambda_r - \lambda_h}de^{-\lambda_c t} - \int_0^\infty \frac{\lambda_c(-t^2)}{\lambda_c - \lambda_r - \lambda_h}de^{-(\lambda_r+\lambda_h)t} \\
&= -t^2 e^{-\lambda_c t}\Big|_0^\infty + \int_0^\infty 2te^{-\lambda_c t}dt - \frac{\lambda_c t^2 e^{-\lambda_r t}}{\lambda_c - \lambda_r}\Big|_0^\infty + \int_0^\infty \frac{2\lambda_c te^{-\lambda_r t}}{\lambda_c - \lambda_r}dt + \frac{\lambda_c t^2 e^{-\lambda_c t}}{\lambda_c - \lambda_r}\Big|_0^\infty \\
&\quad - \int_0^\infty \frac{2\lambda_c te^{-\lambda_c t}}{\lambda_c - \lambda_r}dt - \frac{\lambda_c t^2 e^{-\lambda_h t}}{\lambda_c - \lambda_h}\Big|_0^\infty + \int_0^\infty \frac{2\lambda_c te^{-\lambda_h t}}{\lambda_c - \lambda_h}dt + \frac{\lambda_c t^2 e^{-\lambda_c t}}{\lambda_c - \lambda_h}\Big|_0^\infty - \int_0^\infty \frac{2\lambda_c te^{-\lambda_c t}}{\lambda_c - \lambda_h}dt \\
&\quad + \frac{\lambda_c t^2 e^{-(\lambda_h+\lambda_r)t}}{\lambda_c - \lambda_h - \lambda_r}\Big|_0^\infty - \int_0^\infty \frac{2\lambda_c te^{-(\lambda_h+\lambda_r)t}}{\lambda_c - \lambda_h - \lambda_r}dt - \frac{\lambda_c t^2 e^{-\lambda_c t}}{\lambda_c - \lambda_h - \lambda_r}\Big|_0^\infty + \int_0^\infty \frac{2\lambda_c te^{-\lambda_c t}}{\lambda_c - \lambda_h - \lambda_r}dt \\
&= \frac{2}{\lambda_c^2} + \frac{2\lambda_c}{(\lambda_c - \lambda_r)\lambda_r^2} - \frac{2\lambda_c}{(\lambda_c - \lambda_r)\lambda_c^2} + \frac{2\lambda_c}{(\lambda_c - \lambda_h)\lambda_h^2} - \frac{2\lambda_c}{(\lambda_c - \lambda_h)\lambda_c^2} - \frac{2\lambda_c}{(\lambda_c - \lambda_r - \lambda_h)(\lambda_r + \lambda_h)^2} \\
&\quad + \frac{2\lambda_c}{(\lambda_c - \lambda_r - \lambda_h)\lambda_c^2} \\
&= \frac{2}{\lambda_c^2} + \frac{2(\lambda_c + \lambda_r)}{\lambda_c \lambda_r^2} + \frac{2(\lambda_c + \lambda_h)}{\lambda_c \lambda_h^2} - \frac{2(\lambda_c + \lambda_h + \lambda_r)}{\lambda_c(\lambda_r + \lambda_h)^2}.
\end{aligned} \tag{A.5}$$

If any inequality in (A.1) becomes an equality, from (A.4), we have

$$\begin{aligned}
-\lambda_c \int_0^\infty t^2 e^{-\lambda_c t}(1-\lambda_c t)dt &= -\lambda_c \int_0^\infty t^2 e^{-\lambda_c t}dt + \lambda_c^2 \int_0^\infty t^3 e^{-\lambda_c t}dt \\
&= -\lambda_c \int_0^\infty t^2 e^{-\lambda_c t}dt - \lambda_c t^3 e^{-\lambda_c t}\Big|_0^\infty + \int_0^\infty e^{-\lambda_c t}dt^3 \\
&= 2\lambda_c \int_0^\infty t^2 e^{-\lambda_c t}dt = \frac{4}{\lambda_c^2},
\end{aligned}$$

where the derivation of the last equality is similar to those in (A.5). Thus, the same expression to (A.5) can be derived even if any inequality in (A.1) becomes an equality.

Next we calculate flow time variance Var.

$$\begin{aligned}
Var = E(t^2) - T^2 &= \frac{2}{\lambda_c^2} + \frac{2(\lambda_c+\lambda_r)}{\lambda_c\lambda_r^2} + \frac{2(\lambda_c+\lambda_h)}{\lambda_c\lambda_h^2} - \frac{2(\lambda_c+\lambda_h+\lambda_r)}{\lambda_c(\lambda_r+\lambda_h)^2} - \Big(\frac{1}{\lambda_c}+\frac{1}{\lambda_r}+\frac{1}{\lambda_h}-\frac{1}{\lambda_r+\lambda_h}\Big)^2 \\
&= \frac{2}{\lambda_c^2} + \frac{2(\lambda_c+\lambda_r)}{\lambda_c\lambda_r^2} + \frac{2(\lambda_c+\lambda_h)}{\lambda_c\lambda_h^2} - \frac{2(\lambda_c+\lambda_h+\lambda_r)}{\lambda_c(\lambda_r+\lambda_h)^2} - \frac{1}{\lambda_c^2} - \frac{1}{\lambda_r^2} - \frac{1}{\lambda_h^2} - \frac{2}{\lambda_c\lambda_r} - \frac{2}{\lambda_c\lambda_h} - \frac{2}{\lambda_r\lambda_h} \\
&\quad + \frac{2}{\lambda_c(\lambda_h+\lambda_r)} + \frac{2}{\lambda_r(\lambda_h+\lambda_r)} + \frac{2}{\lambda_h(\lambda_h+\lambda_r)} - \frac{1}{(\lambda_r+\lambda_h)^2} \\
&= \frac{1}{\lambda_h^2} + \frac{1}{\lambda_r^2} + \frac{1}{\lambda_c^2} + \frac{2}{\lambda_r(\lambda_r+\lambda_h)} + \frac{2}{\lambda_h(\lambda_r+\lambda_h)} - \frac{3}{(\lambda_r+\lambda_h)^2} - \frac{2}{\lambda_r\lambda_h} \\
&= \frac{1}{\lambda_h^2} + \frac{1}{\lambda_r^2} + \frac{1}{\lambda_c^2} - \frac{3}{(\lambda_r+\lambda_h)^2}.
\end{aligned}$$

Then the CV of flow time follows.

$$CV = \frac{\sqrt{Var}}{T} = \frac{\sqrt{\frac{1}{\lambda_h^2}+\frac{1}{\lambda_r^2}+\frac{1}{\lambda_c^2}-\frac{3}{(\lambda_r+\lambda_h)^2}}}{\frac{1}{\lambda_c}+\frac{1}{\lambda_r}+\frac{1}{\lambda_h}-\frac{1}{\lambda_r+\lambda_h}}.$$

■

Proof of Theorem 2: From assumptions (i)-(v), random processes R and H follow phase-type distribution $PH(\boldsymbol{\alpha}_r, \boldsymbol{B}_r)$ and $PH(\boldsymbol{\alpha}_h, \boldsymbol{B}_h)$, with orders m_r and m_h, respectively. Define process $X_1 = \max(R, H)$, i.e., X_1 finishes only after both H and R finish. From Theorem 3.18 in Verbelen (2013), X_1 also follows a phase-type distribution $PH(\boldsymbol{\alpha}_1, \boldsymbol{B}_1)$, whose order m_1 and parameters $\boldsymbol{\alpha}_1$ and $\boldsymbol{B}_1$ are defined as

$$\begin{aligned}
m_1 &= m_h m_r + m_h + m_r, \\
\boldsymbol{\alpha}_1 &= (\boldsymbol{\alpha}_h \otimes \boldsymbol{\alpha}_r, \boldsymbol{\alpha}_h \alpha_{r,m_r+1}, \boldsymbol{\alpha}_r \alpha_{h,m_h+1}), \\
\boldsymbol{B}_1 &= \begin{bmatrix} \boldsymbol{B}_h \oplus \boldsymbol{B}_r & \boldsymbol{I}_h \otimes \boldsymbol{b}_r & \boldsymbol{b}_h \otimes \boldsymbol{I}_r \\ \boldsymbol{0} & \boldsymbol{B}_h & \boldsymbol{0} \\ \boldsymbol{0} & \boldsymbol{0} & \boldsymbol{B}_r \end{bmatrix}.
\end{aligned}$$

Here $\oplus$ denotes the Kronecker sum, whose formula is presented in Appendix C.

After finishing process X_1, the joint process C starts. Thus, the total flow time is characterized by process $X = X_1 + C$. From the closure property in phase-type distribution (Theorem 3.16 in Verbelen (2013)), X again follows a phase-type distribution $PH(\boldsymbol{\alpha}, \boldsymbol{B})$ with order $m = m_1 + m_c$, i.e.,

$$m = m_1 + m_c = m_h m_r + m_h + m_r + m_c,$$

and parameter $\boldsymbol{\alpha}$ is defined as

$$\boldsymbol{\alpha} = [\boldsymbol{\alpha}_1, \alpha_{1,m_1+1}\boldsymbol{\alpha}_c] = [\boldsymbol{\alpha}_h \otimes \boldsymbol{\alpha}_r, \boldsymbol{\alpha}_h \alpha_{r,m_r+1}, \boldsymbol{\alpha}_r \alpha_{h,m_h+1}, \alpha_{1,m_1+1}\boldsymbol{\alpha}_c].$$

Let

$$\rho = \alpha_{1,m_1+1} = 1 - \boldsymbol{\alpha}_1 \boldsymbol{1} = 1 - [\boldsymbol{\alpha}_h \otimes \boldsymbol{\alpha}_r, \boldsymbol{\alpha}_h \alpha_{r,m_r+1}, \boldsymbol{\alpha}_r \alpha_{h,m_h+1}]\boldsymbol{1},$$

we have

$$\boldsymbol{\alpha} = [\boldsymbol{\alpha}_h \otimes \boldsymbol{\alpha}_r, \boldsymbol{\alpha}_h \alpha_{r,m_r+1}, \boldsymbol{\alpha}_r \alpha_{h,m_h+1}, \rho\boldsymbol{\alpha}_c].$$

In addition, $\boldsymbol{B}$ is defined as

$$\boldsymbol{B} = \begin{bmatrix} \boldsymbol{B}_1 & \boldsymbol{b}_1\boldsymbol{\alpha}_c \\ \boldsymbol{0} & \boldsymbol{B}_c \end{bmatrix}, \quad \text{where} \quad \boldsymbol{b}_1 = -\boldsymbol{B}_1\boldsymbol{1}. \tag{A.6}$$

Since

$$
\begin{aligned}
(\boldsymbol{B}_h \oplus \boldsymbol{B}_r + \boldsymbol{I}_h \otimes \boldsymbol{b}_r + \boldsymbol{b}_h \otimes \boldsymbol{I}_r)\mathbf{1} &= \boldsymbol{B}_h \otimes \boldsymbol{I}_r\mathbf{1} + \boldsymbol{I}_h \otimes \boldsymbol{B}_r\mathbf{1} + \boldsymbol{I}_h \otimes \boldsymbol{b}_r\mathbf{1} + \boldsymbol{b}_h \otimes \boldsymbol{I}_r\mathbf{1} \\
&= \begin{bmatrix} -\lambda_{h,1}\boldsymbol{I}_r & \lambda_{h,1}\boldsymbol{I}_r & \mathbf{0} & \cdots & \boldsymbol{I} \\ \mathbf{0} & \ddots & \ddots & \ddots & \vdots \\ \vdots & \ddots & -\lambda_{h,i}\boldsymbol{I}_r & \lambda_{h,i}\boldsymbol{I}_r & \vdots \\ \vdots & \ddots & \ddots & \ddots & \vdots \\ \mathbf{0} & \ddots & \ddots & \ddots & -\lambda_{h,m_h}\boldsymbol{I}_r \end{bmatrix} \begin{bmatrix} 1 \\ \vdots \\ 1 \end{bmatrix} + \begin{bmatrix} \boldsymbol{B}_r & \mathbf{0} & \cdots & \mathbf{0} \\ \mathbf{0} & \ddots & \ddots & \vdots \\ \vdots & \ddots & \ddots & \vdots \\ \mathbf{0} & \cdots & \cdots & \boldsymbol{B}_r \end{bmatrix} \begin{bmatrix} 1 \\ \vdots \\ 1 \end{bmatrix} \\
&\quad + \begin{bmatrix} \boldsymbol{b}_r & \mathbf{0} & \cdots & \mathbf{0} \\ \mathbf{0} & \ddots & \ddots & \vdots \\ \vdots & \ddots & \ddots & \vdots \\ \mathbf{0} & \cdots & \cdots & \boldsymbol{b}_r \end{bmatrix} \begin{bmatrix} 1 \\ \vdots \\ 1 \end{bmatrix} + \begin{bmatrix} 0\boldsymbol{I}_r \\ 0\boldsymbol{I}_r \\ \vdots \\ \lambda_{h,m_h}\boldsymbol{I}_r \end{bmatrix} \begin{bmatrix} 1 \\ \vdots \\ 1 \end{bmatrix} \\
&= \begin{bmatrix} 0 \\ 0 \\ \vdots \\ -\lambda_{h,m_h}\boldsymbol{I}_r \end{bmatrix} + \begin{bmatrix} \boldsymbol{B}_r\mathbf{1} \\ \vdots \\ \boldsymbol{B}_r\mathbf{1} \end{bmatrix} + \begin{bmatrix} \boldsymbol{b}_r \\ \vdots \\ \boldsymbol{b}_r \end{bmatrix} + \begin{bmatrix} 0 \\ \vdots \\ \lambda_{h,m_h}\boldsymbol{I}_r \end{bmatrix} = \begin{bmatrix} \boldsymbol{b}_r + \boldsymbol{B}_r\mathbf{1} \\ \vdots \\ \boldsymbol{b}_r + \boldsymbol{B}_r\mathbf{1} \end{bmatrix} = \mathbf{0}.
\end{aligned}
$$

Thus we obtain,

$$
\boldsymbol{b}_1\boldsymbol{\alpha}_c = -\boldsymbol{B}_1\mathbf{1}\boldsymbol{\alpha}_c \begin{bmatrix} -(\boldsymbol{B}_h \oplus \boldsymbol{B}_r + \boldsymbol{I}_h \otimes \boldsymbol{b}_r + \boldsymbol{b}_h \otimes \boldsymbol{I}_r)\mathbf{1}\boldsymbol{\alpha}_c \\ -\boldsymbol{B}_h\mathbf{1}\boldsymbol{\alpha}_c \\ -\boldsymbol{B}_r\mathbf{1}\boldsymbol{\alpha}_c \end{bmatrix} = \begin{bmatrix} \mathbf{0} \\ \boldsymbol{b}_h\boldsymbol{\alpha}_c \\ \boldsymbol{b}_r\boldsymbol{\alpha}_c \end{bmatrix}.
$$

Using these parameters, from Theorem 3.11 in Verbelen (2013), the cumulative distribution function of the continuous phase-type distribution $X \sim PH(\boldsymbol{\alpha}, \boldsymbol{B})$ is given by

$$
P(X \leq t) = 1 - \boldsymbol{\alpha}e^{\boldsymbol{B}t}\mathbf{1}. \tag{A.7}
$$

Thus, given time period T_d, the service rate $S(T_d)$ follows:

$$
S(T_d) = 1 - \boldsymbol{\alpha}e^{\boldsymbol{B}T_d}\mathbf{1}. \tag{A.8}
$$

■

Proof of Corollary 3: From the cumulative density function defined in (A.7), the probability density function $s(t)$ will be

$$
s(t) = \begin{cases} 0, & t = 0, \\ \boldsymbol{\alpha}e^{\boldsymbol{B}t}\boldsymbol{b}, & t > 0. \end{cases} \tag{A.9}
$$

From Corollary 3.14 in Verbelen (2013), The k-th noncentral moments of the continuous PH distribution $PH(\boldsymbol{\alpha}, \boldsymbol{B})$ can be derived as follows:

$$
E(t^k) = (-1)^k k!\boldsymbol{\alpha}\boldsymbol{B}^{-k}\mathbf{1}. \tag{A.10}
$$

When $k = 1$, we obtain

$$
T = E(t) = -\boldsymbol{\alpha}\boldsymbol{B}^{-1}\mathbf{1}.
$$

■

Proof of Corollary 4: From (A.10),

$$
E(t^2) = 2\boldsymbol{\alpha}\boldsymbol{B}^{-2}\mathbf{1}.
$$

It follows that

$$Var = E(t^2) - (E(t))^2 = 2\boldsymbol{\alpha}\boldsymbol{B}^{-2}\mathbf{1} - (\boldsymbol{\alpha}\boldsymbol{B}^{-1}\mathbf{1})^2.$$

Thus,

$$CV = \frac{\sqrt{Var}}{T} = \frac{\sqrt{2\boldsymbol{\alpha}\boldsymbol{B}^{-2}\mathbf{1} - (\boldsymbol{\alpha}\boldsymbol{B}^{-1}\mathbf{1})^2}}{-\boldsymbol{\alpha}\boldsymbol{B}^{-1}\mathbf{1}}.$$

■

Appendix B: Proofs for Section 4

Proof of Proposition 1:

$$\begin{aligned}
\frac{\partial T}{\partial \lambda_r} &= -\frac{1}{\lambda_r^2} + \frac{1}{(\lambda_r+\lambda_h)^2} = -\frac{\lambda_h(\lambda_h+2\lambda_r)}{\lambda_r^2(\lambda_h+\lambda_r)^2} < 0,\\
\frac{\partial T}{\partial \lambda_h} &= -\frac{1}{\lambda_h^2} + \frac{1}{(\lambda_r+\lambda_h)^2} = -\frac{\lambda_r(\lambda_r+2\lambda_h)}{\lambda_h^2(\lambda_h+\lambda_r)^2} < 0,\\
\frac{\partial T}{\partial \lambda_c} &= -\frac{1}{\lambda_c^2} < 0.
\end{aligned}$$

Thus T is monotonically decreasing in λ_r, λ_h, and λ_c. ■

Proof of Proposition 2:

$$\begin{aligned}
\frac{\partial CV}{\partial \lambda_c} &= \frac{\partial \frac{\sqrt{\frac{1}{\lambda_h^2}+\frac{1}{\lambda_r^2}+\frac{1}{\lambda_c^2}-\frac{3}{(\lambda_r+\lambda_h)^2}}}{\frac{1}{\lambda_c}+\frac{1}{\lambda_r}+\frac{1}{\lambda_h}-\frac{1}{\lambda_r+\lambda_h}}}{\partial \lambda_c}\\
&= \frac{\frac{1}{2}(\frac{1}{\lambda_h^2}+\frac{1}{\lambda_r^2}+\frac{1}{\lambda_c^2}-\frac{3}{(\lambda_r+\lambda_h)^2})^{-\frac{1}{2}}(-2)\frac{1}{\lambda_c^3}}{\frac{1}{\lambda_c}+\frac{1}{\lambda_r}+\frac{1}{\lambda_h}-\frac{1}{\lambda_r+\lambda_h}} - \frac{(\frac{1}{\lambda_h^2}+\frac{1}{\lambda_r^2}+\frac{1}{\lambda_c^2}-\frac{3}{(\lambda_r+\lambda_h)^2})^{\frac{1}{2}}(-1)(-\frac{1}{\lambda_c^2})}{(\frac{1}{\lambda_c}+\frac{1}{\lambda_r}+\frac{1}{\lambda_h}-\frac{1}{\lambda_r+\lambda_h})^2}\\
&= \frac{-(\frac{1}{\lambda_h^2}+\frac{1}{\lambda_r^2}+\frac{1}{\lambda_c^2}-\frac{3}{(\lambda_r+\lambda_h)^2})^{-\frac{1}{2}}}{\lambda_c^2(\frac{1}{\lambda_c}+\frac{1}{\lambda_r}+\frac{1}{\lambda_h}-\frac{1}{\lambda_r+\lambda_h})^2}\Big[\frac{1}{\lambda_c}\Big(\frac{1}{\lambda_c}+\frac{1}{\lambda_r}+\frac{1}{\lambda_h}-\frac{1}{\lambda_r+\lambda_h}\Big)+\frac{1}{\lambda_h^2}+\frac{1}{\lambda_r^2}+\frac{1}{\lambda_c^2}-\frac{3}{(\lambda_r+\lambda_h)^2}\Big]\\
&< 0,\\
\frac{\partial CV}{\partial \lambda_r} &= \frac{\partial \frac{\sqrt{\frac{1}{\lambda_h^2}+\frac{1}{\lambda_r^2}+\frac{1}{\lambda_c^2}-\frac{3}{(\lambda_r+\lambda_h)^2}}}{\frac{1}{\lambda_c}+\frac{1}{\lambda_r}+\frac{1}{\lambda_h}-\frac{1}{\lambda_r+\lambda_h}}}{\partial \lambda_r}\\
&= \frac{\frac{1}{2}(\frac{1}{\lambda_h^2}+\frac{1}{\lambda_r^2}+\frac{1}{\lambda_c^2}-\frac{3}{(\lambda_r+\lambda_h)^2})^{-\frac{1}{2}}[\frac{-2}{\lambda_r^3}-\frac{-6}{(\lambda_r+\lambda_h)^3}]}{\frac{1}{\lambda_c}+\frac{1}{\lambda_r}+\frac{1}{\lambda_h}-\frac{1}{\lambda_r+\lambda_h}} - \frac{(\frac{1}{\lambda_h^2}+\frac{1}{\lambda_r^2}+\frac{1}{\lambda_c^2}-\frac{3}{(\lambda_r+\lambda_h)^2})^{\frac{1}{2}}(\frac{1}{\lambda_r^2}-\frac{1}{(\lambda_h+\lambda_r)^2})}{(\frac{1}{\lambda_c}+\frac{1}{\lambda_r}+\frac{1}{\lambda_h}-\frac{1}{\lambda_r+\lambda_h})^2}\\
&= \frac{-(\frac{1}{\lambda_h^2}+\frac{1}{\lambda_r^2}+\frac{1}{\lambda_c^2}-\frac{3}{(\lambda_r+\lambda_h)^2})^{-\frac{1}{2}}}{(\frac{1}{\lambda_c}+\frac{1}{\lambda_r}+\frac{1}{\lambda_h}-\frac{1}{\lambda_r+\lambda_h})^2}\Big[\Big(\frac{1}{\lambda_r^3}+\frac{3}{(\lambda_h+\lambda_r)^3}\Big)\Big(\frac{1}{\lambda_c}+\frac{1}{\lambda_r}+\frac{1}{\lambda_h}-\frac{1}{\lambda_r+\lambda_h}\Big)\\
&\quad+\Big(\frac{1}{\lambda_h^2}+\frac{1}{\lambda_r^2}+\frac{1}{\lambda_c^2}-\frac{3}{(\lambda_r+\lambda_h)^2}\Big)\Big(\frac{1}{\lambda_r^2}-\frac{1}{(\lambda_r+\lambda_h)^2}\Big)\Big]\\
&< 0.
\end{aligned}$$

Analogously, by switching λ_r and λ_h, we have

$$\frac{\partial CV}{\partial \lambda_h} < 0.$$

Thus CV is monotonically decreasing in λ_r, λ_h, and λ_c. ■

Proof of Proposition 3: Define

$$L(\lambda_h, \lambda_r, \beta) = \frac{1}{\lambda_h} + \frac{1}{\lambda_r} - \frac{1}{\lambda_r + \lambda_h} + \beta\Big(T_{prep} - \frac{1}{\lambda_r} - \frac{1}{\lambda_h}\Big).$$

It follows that

$$\frac{\partial L}{\partial \lambda_h} = -\frac{1}{\lambda_h^2} + \frac{1}{(\lambda_r + \lambda_h)^2} + \frac{\beta}{\lambda_h^2},$$
$$\frac{\partial L}{\partial \lambda_r} = -\frac{1}{\lambda_r^2} + \frac{1}{(\lambda_r + \lambda_h)^2} + \frac{\beta}{\lambda_r^2}.$$

Now let

$$\frac{\partial L}{\partial \lambda_h} = \frac{\partial L}{\partial \lambda_r} = 0,$$

we obtain

$$\lambda_h = \lambda_r.$$

■

Proof of Proposition 4: From the proof of Proposition 1, we obtain

$$\Big|\frac{\partial T}{\partial \lambda_r}\Big| - \Big|\frac{\partial T}{\partial \lambda_h}\Big| = \frac{\lambda_h(\lambda_h + 2\lambda_r)}{\lambda_r^2(\lambda_h + \lambda_r)^2} - \frac{\lambda_r(\lambda_r + 2\lambda_h)}{\lambda_h^2(\lambda_h + \lambda_r)^2} = \frac{(\lambda_r^2 + \lambda_h^2)(\lambda_h^2 - \lambda_r^2) + 2\lambda_r\lambda_h(\lambda_h^2 - \lambda_r^2)}{\lambda_h^2\lambda_r^2(\lambda_h + \lambda_r)^2}$$
$$= \frac{(\lambda_h + \lambda_r)^2(\lambda_h^2 - \lambda_r^2)}{\lambda_h^2\lambda_r^2(\lambda_h + \lambda_r)^2} = \frac{1}{\lambda_r^2} - \frac{1}{\lambda_h^2}.$$

Thus, when λ_r is smaller (i.e., larger $\frac{1}{\lambda_r}$), the difference is positive, and vice versa. Then the argument follows. ■

Proof of Proposition 5: Similar to the proof of Proposition 4, when $i = r$, we have

$$\Big|\frac{\partial T}{\partial \lambda_r}\Big| - \Big|\frac{\partial T}{\partial \lambda_c}\Big| = \frac{\lambda_h(\lambda_h + 2\lambda_r)}{\lambda_r^2(\lambda_h + \lambda_r)^2} - \frac{1}{\lambda_c^2} = \frac{\lambda_h^2 + 2\lambda_r\lambda_h + \lambda_r^2 - \lambda_r^2}{\lambda_r^2(\lambda_h + \lambda_r)^2} - \frac{1}{\lambda_c^2}$$
$$= \frac{1}{\lambda_r^2} - \frac{1}{(\lambda_h + \lambda_r)^2} - \frac{1}{\lambda_c^2}.$$

Thus, $\Big|\frac{\partial T}{\partial \lambda_r}\Big| \geq \Big|\frac{\partial T}{\partial \lambda_c}\Big|$ is equivalent to $\frac{1}{\lambda_r^2} \geq \frac{1}{(\lambda_h+\lambda_r)^2} + \frac{1}{\lambda_c^2}$. Similar argument applies to $i = h$. ■

Proof of Proposition 6: From Corollary 3, expressions in (A.6),

$$T = -\boldsymbol{\alpha}\boldsymbol{B}^{-1}\mathbf{1} = -\boldsymbol{\alpha}\begin{bmatrix} \boldsymbol{B}_1 & \boldsymbol{b}_1\boldsymbol{\alpha}_c \\ \mathbf{0} & \boldsymbol{B}_c \end{bmatrix}^{-1}\mathbf{1} = -\boldsymbol{\alpha}\begin{bmatrix} \boldsymbol{B}_1^{-1} & -\boldsymbol{B}_1^{-1}\boldsymbol{b}_1\boldsymbol{\alpha}_c\boldsymbol{B}_c^{-1} \\ \mathbf{0} & \boldsymbol{B}_c^{-1} \end{bmatrix}\mathbf{1} = -\boldsymbol{\alpha}\begin{bmatrix} \boldsymbol{B}_1^{-1} & \mathbf{1}\boldsymbol{\alpha}_c\boldsymbol{B}_c^{-1} \\ \mathbf{0} & \boldsymbol{B}_c^{-1} \end{bmatrix}\mathbf{1}$$
$$= -\boldsymbol{\alpha}\begin{bmatrix} \boldsymbol{B}_1^{-1}\mathbf{1} + \mathbf{1}\boldsymbol{\alpha}_c\boldsymbol{B}_c^{-1}\mathbf{1} \\ \boldsymbol{B}_c^{-1}\mathbf{1} \end{bmatrix} = -\boldsymbol{\alpha}\begin{bmatrix} \boldsymbol{B}_1^{-1}\mathbf{1} \\ \mathbf{0} \end{bmatrix} - \boldsymbol{\alpha}\begin{bmatrix} \mathbf{1}\boldsymbol{\alpha}_c \\ \boldsymbol{I} \end{bmatrix}\boldsymbol{B}_c^{-1}\mathbf{1} = -\boldsymbol{\alpha}\begin{bmatrix} \boldsymbol{B}_1^{-1}\mathbf{1} \\ \mathbf{0} \end{bmatrix} - \boldsymbol{\alpha}\boldsymbol{B}_c^{-1}\mathbf{1}.$$

For the monotonicity with respect to $\lambda_{c,j}$, $j = 1, \ldots, m_c$, since $\boldsymbol{B}_1^{-1}\mathbf{1}$ is independent of $\lambda_{c,j}$, only the second

term $-\boldsymbol{\alpha}\boldsymbol{B}_c^{-1}\mathbf{1}$ needs to be considered. Thus, we have

$$\boldsymbol{B}_c^{-1} = \begin{bmatrix} -\lambda_{c,1} & \lambda_{c,1} & 0 & \cdots & 0 \\ 0 & -\lambda_{c,2} & \lambda_{c,2} & \ddots & 0 \\ 0 & \ddots & \ddots & \ddots & \vdots \\ 0 & \ddots & \ddots & -\lambda_{c,m_{c-1}} & \lambda_{c,m_{c-1}} \\ 0 & \ddots & \ddots & \ddots & -\lambda_{c,m_c} \end{bmatrix}^{-1} = \begin{bmatrix} -\frac{1}{\lambda_{c,1}} & -\frac{1}{\lambda_{c,2}} & -\frac{1}{\lambda_{c,3}} & \cdots & -\frac{1}{\lambda_{c,m_c}} \\ 0 & -\frac{1}{\lambda_{c,2}} & -\frac{1}{\lambda_{c,3}} & \ddots & -\frac{1}{\lambda_{c,m_c}} \\ 0 & \ddots & \ddots & \ddots & \vdots \\ 0 & \ddots & \ddots & -\frac{1}{\lambda_{c,m_{c-1}}} & -\frac{1}{\lambda_{c,m_c}} \\ 0 & \ddots & \ddots & \ddots & -\frac{1}{\lambda_{c,m_c}} \end{bmatrix}.$$

It follows that

$$-\boldsymbol{\alpha}\boldsymbol{B}_c^{-1}\mathbf{1} = \begin{bmatrix} -1 & 0 \cdots & 0 \end{bmatrix} \cdot \begin{bmatrix} -\frac{1}{\lambda_{c,1}} & -\frac{1}{\lambda_{c,2}} & \cdots & -\frac{1}{\lambda_{c,m_c}} \\ 0 & -\frac{1}{\lambda_{c,2}} & \ddots & -\frac{1}{\lambda_{c,m_c}} \\ 0 & \ddots & \ddots & \vdots \\ 0 & \ddots & \ddots & -\frac{1}{\lambda_{c,m_c}} \end{bmatrix} \cdot \begin{bmatrix} 1 \\ 1 \\ \vdots \\ 1 \end{bmatrix}$$

$$= \begin{bmatrix} \frac{1}{\lambda_{c,1}} & \frac{1}{\lambda_{c,2}} & \cdots & \frac{1}{\lambda_{c,m_c}} \end{bmatrix} \cdot \begin{bmatrix} 1 \\ 1 \\ \vdots \\ 1 \end{bmatrix} = \sum_{j=1}^{m_c} \frac{1}{\lambda_{c,j}}.$$

Thus

$$\frac{\partial T}{\partial \lambda_{c,i}} = -\frac{1}{\lambda_{c,i}^2} < 0.$$

The expected flow time of the system is monotonically decreasing with respect to $\lambda_{c,i}$. ■

Proof Proposition 7: Similar to the proof of Proposition 3, define

$$L(\lambda_{h,1}, \ldots, \lambda_{h,m_h}, \lambda_{r,1}, \ldots, \lambda_{r,m_r}, \beta) = -\boldsymbol{\alpha}\boldsymbol{B}^{-1}\mathbf{1} + \beta\Big(T_{prep} - \sum_{j=1}^{m_r} \frac{1}{\lambda_{r,j}} - \sum_{j=1}^{m_h} \frac{1}{\lambda_{h,j}}\Big).$$

It follows that

$$\frac{\partial L}{\partial \lambda_{r,j}} = -\frac{\partial \boldsymbol{\alpha} \begin{bmatrix} \boldsymbol{B}_1^{-1}\mathbf{1} \\ \mathbf{0} \end{bmatrix}}{\partial \lambda_{r,j}} + \frac{\beta}{\lambda_{r,j}^2},$$

$$\frac{\partial L}{\partial \lambda_{h,j}} = -\frac{\partial \boldsymbol{\alpha} \begin{bmatrix} \boldsymbol{B}_1^{-1}\mathbf{1} \\ \mathbf{0} \end{bmatrix}}{\partial \lambda_{h,j}} + \frac{\beta}{\lambda_{h,j}^2}.$$

Now let

$$\frac{\partial L}{\partial \lambda_{r,j}} = \frac{\partial L}{\partial \lambda_{h,j}} = 0,$$

we need to have

$$m_r = m_h, \qquad \lambda_{h,j} = \lambda_{r,j}, \quad j = 1, \ldots, m_r.$$

■

Proof of Proposition 8: When $\lambda_{c,k} \geq \lambda_{c,j}$, it immediately follows that

$$\left|\frac{\partial T}{\lambda_{c,j}}\right| - \left|\frac{\partial T}{\lambda_{c,k}}\right| = \frac{1}{\lambda_{c,j}^2} - \frac{1}{\lambda_{c,k}^2} \geq 0.$$

■

Appendix C: Kronecker Product and Sum

If $\boldsymbol{X}$ is an $m \times n$ matrix and $\boldsymbol{Y}$ is a $p \times q$ matrix, then the Kronecker product $\boldsymbol{X} \otimes \boldsymbol{Y}$ is a $pm \times qn$ block matrix:

$$\boldsymbol{X} \otimes \boldsymbol{Y} = \begin{bmatrix} x_{11}\boldsymbol{Y} & \cdots & x_{1n}\boldsymbol{Y} \\ \vdots & \ddots & \vdots \\ x_{m1}\boldsymbol{Y} & \cdots & x_{mn}\boldsymbol{Y} \end{bmatrix} = \begin{bmatrix} x_{11}y_{11} & \cdots & x_{11}y_{1q} & \cdots & x_{1n}y_{11} & \cdots & x_{1n}y_{1q} \\ \vdots & \ddots & \vdots & & \vdots & \ddots & \vdots \\ x_{11}y_{p1} & \cdots & x_{11}y_{pq} & \cdots & x_{1n}y_{p1} & \cdots & x_{1n}y_{pq} \\ \vdots & & \vdots & \ddots & \vdots & & \vdots \\ x_{m1}y_{11} & \cdots & x_{m1}y_{1q} & \cdots & x_{mn}y_{11} & \cdots & x_{mn}y_{1q} \\ \vdots & \ddots & \vdots & & \vdots & \ddots & \vdots \\ x_{m1}y_{p1} & \cdots & x_{m1}y_{pq} & \cdots & x_{mn}y_{p1} & \cdots & x_{mn}y_{pq} \end{bmatrix}. \quad \text{(C.1)}$$

When $\boldsymbol{X} = [x]_n$ and $\boldsymbol{Y} = [y]_q$ are square matrices with dimensions n and q, respectively, the Kronecker sum of $\boldsymbol{X}$ and $\boldsymbol{Y}$ is denoted as $\boldsymbol{X} \oplus \boldsymbol{Y}$, which can be calculated as

$$\boldsymbol{X} \oplus \boldsymbol{Y} = (\boldsymbol{X} \otimes \boldsymbol{I}_q) + (\boldsymbol{I}_n \otimes \boldsymbol{Y}). \quad \text{(C.2)}$$

References

Altiok, T. and Perros, H.G. (1986). Open networks of queues with blocking: split and merge configurations. *IIE Transactions*, **18** (3), 251–261.

Bauer, A., Wollherr, D. and Buss, M. (2008). Human–robot collaboration: a survey. *International Journal of Humanoid Robotics*, **5** (1), 47–66.

Bolmsjo, G., Danielsson, F. and Svensson, B. (2012). Collaborative robots to support flexible operation in a manufacturing system. *Proceedings of the 22nd International Conference on Flexible Automation and Intelligent Manufacturing*, 531–538.

Buzacott, J.A. and Shanthikumar, J.G. (1993). *Stochastic Models of Manufacturing Systems*, Prentice Hall, Englewood Cliffs, NJ.

Chandrasekaran, B. and Conrad, J.M. (2015). Human-robot collaboration: a survey. *SoutheastCon 2015*, Fort Lauderdale, FL, 1–8.

Chen, F., Sekiyama, K., Cannella, F. and Fukuda, T. (2013). Optimal subtask allocation for human and robot collaboration within hybrid assembly system. *IEEE Transactions on Automation Science and Engineering*, **11** (4), 1065–1075.

Chiang, S.-Y., Kuo, C.-T., Lim, J.-T. and Meerkov, S.M. (2000a) Improvability of assembly systems I: problem formulation and performance evaluation. *Mathematical Problems in Engineering*, **6** (4), 321–357.

Chiang, S.-Y., Kuo, C.-T., Lim, J.-T. and Meerkov, S.M. (2000b) Improvability of assembly systems I: improvability indicators and case study. *Mathematical Problems in Engineering*, **6** (4), 359–393.

Collaborative Robots Market Research Report. (2020) https://www.marketsandmarkets.com/Market-Reports/collaborative-robot-market-194541294.html, accessed April 23, 2020.

Dallery, Y. and Gershwin, S.B. (1992). Manufacturing flow line systems: a review of models and analytical results. *Queuing Systems*, **12** (1), 3–94.

Djuric, A.M., Urbanic, R.J. and Rickli, J.L. (2016). A framework for collaborative robot (CoBot) integration in advanced manufacturing systems. *SAE International Journal of Materials and Manufacturing*, **9** (2), 457–464.

El Zaatari, S., Marei, M., Li, W. and Usman, Z. (2019). Cobot programming for collaborative industrial tasks: an overview. *Robotics and Autonomous Systems*, **116**, 162–180.

Faccio, M., Bottin, M. and Rosati, G. (2019). Collaborative and traditional robotic assembly: a comparison model. *The International Journal of Advanced Manufacturing Technology*, **102** (5-8), 1355–1372.

Faccio, M., Minto, R., Rosati, G. and Bottin, M. (2020). The influence of the product characteristics on human-robot collaboration: a model for the performance of collaborative robotic assembly. *The International Journal of Advanced Manufacturing Technology*, **106** (5), 2317–2331.

Fiorini, P.M. and Lipsky, L. (2015). Exact analysis of some split-merge queues. *ACM SIGMETRICS Performance Evaluation Review*, **43** (2), 51–53.

Gershwin, S.B. (1991). Assembly/disassembly systems: an efficient decomposition algorithm for tree-structured networks. *IIE Transactions*, **23** (4), 302–314.

Gershwin, S.B. (1994). *Manufacturing Systems Engineering*, Prentice Hall, Englewood Cliffs, NJ.

Helber, S. and Jusic, H. (2004). A new decomposition approach for non-cyclic continuous material flow lines with a merging flow of material. *Annals of Operations Research*, **125** (1-4), 117–139.

Jia, Z., Zhang, L., Arinez, J. and Xiao, G. (2015). Performance analysis of assembly systems with Bernoulli machines and finite buffers during transients. *IEEE Transactions on Automation Science and Engineering*, **13** (2), 1018–1032.

Ju, F., Li, J. and Deng, W. (2016). Selective assembly system with unreliable Bernoulli machines and finite buffers. *IEEE Transactions on Automation Science and Engineering*, **14** (1), 171–184.

Lang, L. and Arthur, J.L. (1996).Parameter approximation for phase-type distributions. In *Matrix Analytic methods in Stochastic Models*, S. Chakravarthy and A.S. Alfa (eds.), CRC Press.

Lasota, P.A., Fong, T. and Shah, J.A. (2017). A survey of methods for safe human-robot interaction. *Foundations and Trends® in Robotics*, **5** (4), 261–349.

Li, J. (2005). Overlapping decomposition: a system-theoretic method for modeling and analysis of complex manufacturing systems. *IEEE Transactions on Automation Science and Engineering*, **2** (1), 40–53.

Li, J., Blumenfeld, D.E., Huang, N. and Alden, J.A. (2009). Throughput analysis of production systems: recent advances and future topics. *International Journal of Production Research*, **47** (14), 3823–3851.

Li, J. and Meerkov, S.M. (2001). Customer demand satisfaction in production systems: a due-time performance approach. *IEEE Transactions on Robotics and Automation*, **17** (4), 472–482.

Li, J. and Meerkov, S.M. (2005). On the coefficients of variation of uptime and downtime in manufacturing equipment. *Mathematical Problems in Engineering*, **2005**, 1–6.

Li, J. and Meerkov, S.M. (2009). *Production Systems Engineering*, Springer, New York, NY.

Maganha, I., Silva, C., Klement, N., Eynaud, D., Durville, L. and Moniz, S. (2019). Hybrid optimisation approach for sequencing and assignment decision-making in reconfigurable assembly lines. *IFAC-PapersOnLine*, **52** (13), 1367–1372.

Marvel, J.A. (2014). *Collaborative Robots: A Gateway into Factory Automation*, National Institute of Standards and Technology.

Matta, A., Dallery, Y. and Di Mascolo, M. (2005). Analysis of assembly systems controlled with kanbans. *European Journal of Operational Research*, **166** (2), 310–336.

Mokhtarzadeh, M., Tavakkoli-Moghaddam, R., Vahedi-Nouri, B. and Farsi, A. (2020). Scheduling of human-robot collaboration in assembly of printed circuit boards: a constraint programming approach. *International Journal of Computer Integrated Manufacturing*.

Mura, M.D. and G. Dini, G. (2019). Designing assembly lines with humans and collaborative robots: a genetic approach. *CIRP Annals*, **68** (1), 1–4.

Papadopoulos, H.T. and Heavey, C. (1996). Queueing theory in manufacturing systems analysis and design: a classification of models for production and transfer lines. *European Journal of Operational Research*, **92** (1), 1–27.

Papadopolous, H.T., Heavey, C. and Browne, J. (1993). *Queueing Theory in Manufacturing Systems Analysis and Design*, Springer.

Papadopoulos, C.T., Li, J. and O'Kelly, M.E. (2019). A classification and review of timed Markov models of manufacturing systems. *Computers & Industrial Engineering*, **128**, 219–244.

Pearce, M. Mutlu, B., Shah, J. and Radwin, R. (2018). Optimizing makespan and ergonomics in integrating collaborative robots into manufacturing processes. *IEEE Transactions on Automation Science and Engineering*, **15** (4), 1772–1784.

Shih, N.H. (2005). Estimating completion-time distribution in stochastic activity networks. *Journal of the Operational Research Society*, **56** (6), 744–749.

Tsarouchi, P., Matthaiakis, A.-S., Makris, S. and Chryssolouris, G. (2017). On a human-robot collaboration in an assembly cell. *International Journal of Computer Integrated Manufacturing*, **30** (6), 580–589.

Tsimashenka, I. and Knottenbelt, W.J. (2011). Reduction of variability in split-merge systems. In *ICCSW*, 101–107.

Verbelen, R. (2013). *Phase-type Distributions and Mixtures of Erlangs*, Doctoral Dissertation, University of Leuven, Belgium.

Villani, V., Pini, F., Leali, F. and Secchi, C. (2018). Survey on human–robot collaboration in industrial settings: safety, intuitive interfaces and applications. *Mechatronics*, **55**, 248–266.

Viswanadham, N. and Narahari, Y. (1992). *Performance Modeling of Automated Manufacturing Systems*, Prentice Hall, Englewood Cliffs, NJ.

Weckenborg, C., Kieckhafer, K., Muller, C., Grunewald, M. and Spengler, T.S. (2020). Balancing of assembly lines with collaborative robots. *Business Research*, **13**, 93–132.

Zanchettin, A.M., Ceriani, N.M., Rocco, P., Ding, H. and Matthias, B. (2015). Safety in human-robot collaborative manufacturing environments: metrics and control. *IEEE Transactions on Automation Science and Engineering*, **13** (2), 882–893.

Zhao, C. and Li, J. (2014). Analysis and improvement of multi-product assembly systems: an application study at a furniture manufacturing plant. *International Journal of Production Research*, **52** (21), 6399–6413.